Longitudinal Auditory Pathophysiology Following Mild Blast Induced Trauma

Emily X. Han[1,2], Joseph M. Fernandez[2,3], Caitlin Swanberg[2], Riyi Shi[2,3], Edward L. Bartlett[1,2]

[1]Dept. of Biological Sciences, College of Science, Purdue University, West Lafayette, IN

[2]Weldon School of Biomedical Engineering, Purdue University, West Lafayette, IN

[3]Dept. Basic Medical Sciences, College of Veterinary Medicine, Purdue University, West Lafayette, IN

Running head: Longitudinal blast auditory pathophysiology

Correspondence should be addressed to Edward Bartlett (ebartle@purdue.edu)。

Department of Biological Sciences and

The Weldon School of Biomedical Engineering

206 S. Martin Jischke Dr.

Purdue University

West Lafayette, Indiana 47907-1791

Keywords: Blast, traumatic brain injury, envelope following response, neurodegeneration, auditory evoked potentials

Abstract

Blast-induced hearing difficulties affect thousands of veterans and civilians. The long-term impact of even a mild blast exposure on the central auditory system is hypothesized to contribute to lasting behavioral complaints associated with mild blast traumatic brain injury (bTBI). Although recovery from mild blast has been studied separately over brief or long time windows, few, if any, studies have investigated recovery longitudinally over short-term and longer-term (months) time windows. Specifically, many peripheral measures of auditory function either recover or exhibit subclinical deficits, masking deficits in processing complex, real-world stimuli that may recover differently. Thus, examining the acute time course and pattern of neurophysiological impairment using appropriate stimuli is critical to better understanding and intervention of bTBI-induced auditory system impairments. Here, we compared auditory brainstem response, middle-latency auditory evoked potentials, and envelope following responses. Stimuli were clicks, tone pips, amplitude modulated tones in quiet and in noise, and speech-like stimuli (iterated rippled noise pitch contours) in adult male rats subjected to mild blast and sham exposure over the course of two months. We found that blast animals demonstrated drastic threshold increases and auditory transmission deficits immediately after blast exposure, followed by substantial recovery during the window of 7-14 days post-blast, though with some deficits remaining even after two months. Challenging conditions and speech-like stimuli can better elucidate mild bTBI-induced auditory deficit during this period. Our

results suggest multiphasic recovery and therefore potentially different time windows for treatment, and deficits can be best observed using a small battery of sound stimuli.

New and Noteworthy

Few studies on blast-induced hearing deficits go beyond simple sounds or two times post-exposure. Therefore, the recovery arc for potential therapies and real-world listening is poorly understood. Evidence suggested multiple recovery phases over 2 months post-exposure. Hearing thresholds largely recovered within 14 days and partially explained recovery. However, mid-latency responses, responses to AM in noise, and speech-like pitch sweeps all exhibited extended changes, implying persistent central auditory deficits and the importance of subclinical threshold shifts.

Introduction

Hearing loss stands out as one of the most commonly reported consequences following blast injuries and can last for months or even years without significant external injury (Cohen et al. 2002; Cave et al. 2007; Ritenour et al. 2008; Saunders et al. 2015). Hearing difficulties have been hypothesized to contribute to many behavioral complaints associated with mild blast traumatic brain injury (Gallun et al. 2012b; Vander Werff 2012). Most studies regarding blast-induced hearing loss have focused on damage in different parts of the peripheral auditory system (PAS) (Kerr 1980; DePalma et al. 2005). However, significant hearing difficulties can occur in the absence of peripheral diagnostic indicators such as eardrum rupture or clinical threshold shifts (hearing loss >25 dB), indicating potential disruptions further upstream (Remenschneider et al. 2014; Saunders et al. 2015; Van Haesendonck et al. 2018). Increasing clinical (Berger et al. 1997; Cohen et al. 2002; Cave et al. 2007; Ritenour et al. 2008; Lew et al. 2009; Gallun et al. 2012a) and laboratory (Patterson and Hamernik 1997; Ewert et al. 2012; Cho et al. 2013b; Du et al. 2013; Masri et al. 2018) evidence suggest that both peripheral and central auditory system (CAS) are important blast-susceptible structures, where CAS includes the brainstem, midbrain, thalamus, and cortex.

Subcortical CAS such as the auditory brainstem may be particularly vulnerable to blast injury, including hemorrhages, intracranial deformation and blood-brain barrier (BBB) permeability, glutamate excitotoxicity, elevated calcium, as well as elevated markers of oxidative stress and neuroinflammation from near short-term (1-7 days) up to 2 weeks (Knudsen and Øen 2003; Leung et al. 2008; Säljö et al. 2011; Cho et al. 2013a; Song et al.

2015; Walls et al. 2016). Functional changes, such as spontaneous hyperactivity in the auditory brainstem (Luo et al. 2014a, 2014b), as well as structural changes in OHC loss (Ewert et al. 2012), axonal integrity, white matter changes in the inferior colliculus (IC) and auditory thalamus (Mao et al. 2012a), have been shown post-blast at various time points, from 24 hours, 7 days up to 2-3 weeks. Most of these previous studies only assessed one or two time points post-blast. Given the likelihood of multiple phases of primary and secondary blast-induced damage and their corresponding anatomical and electrophysiological changes, understanding the trajectory of post-blast recovery can help to identify critical time points and to direct therapies that are matched to the recovery mechanisms at those time points.

Clinical reports have suspected “hidden hearing loss” in blast-exposed veterans due to deficits in suprathreshold auditory processing with minimal changes in auditory thresholds (Gallun et al. 2012a; Saunders et al. 2015; Bressler et al. 2017). This occurs in age-related or noise-induced sensorineural hearing loss and encompasses putative changes resulting from hair cell or auditory nerve/synapse damage (Hickox and Liberman 2014; Plack et al. 2014; Bharadwaj et al. 2015; Kujawa and Liberman 2015; Viana et al. 2015; Liberman 2017). One consequence could be CAS adaptations in response to peripheral deafferentation (Caspary et al. 2005, 2008; Wang et al. 2009), which has been speculated to impair temporal processing (Walton 2010; Parthasarathy and Bartlett 2011, 2012; Rabang et al. 2012). Blast studies on human subjects often used speech and complex temporally modulated stimuli to pin down “hidden” temporal processing losses

that were not apparent with simple audiological measures (Gallun et al. 2012b; Saunders et al. 2015; Bressler et al. 2017; Kubli et al. 2018). However, blast studies in animals rarely go beyond simple auditory stimuli such as clicks, tones and AM modulation in a quiet background (Ewert et al. 2012; Race et al. 2017; Masri et al. 2018).

Using the same rat model as our previous publication (Race et al. 2017), our study documents a detailed time course of blast-induced hearing loss recovery in the subcortical CAS using auditory evoked potentials (AEPs). We specifically chose Iterated Rippled Noise (IRN) with pitch sweep alongside Amplitude Modulation (AM) stimuli in quiet and in modulated noise as temporally complex stimuli in assessing the processing of temporal attributes. IRN was used in neurophysiological and behavioral studies in both human (Krishnan et al. 2014, 2015; Peter et al. 2014; Wagner et al. 2017; Shearer et al. 2018) and animal models (Bendor and Wang 2005; Alsindi et al. 2018), creating "pseudo-pitch" pitch contours with broadband carriers. IRN bypasses limitations posed by animal frequency range as well as permitting easily adjustable pitch intelligibility by altering the number of noise iterations and thus, the strength of temporal regularity and pitch salience (Patterson et al. 1996).

Materials and Methods

Subject

Male Sprague-Dawley rats (3-4 months) were assigned into Sham group and Blast group randomly. A total of 11 Sham animals and 13 blast animals were used in this study. All animals were kept and raised in relatively quiet and standard laboratory animal housing

120 conditions. All protocols were approved by the Purdue Animals Care and Use Committee
121 (PACUC #1111000280).
122
123 **Blast Exposure**
124 Animals were anesthetized through intraperitoneal injection of a ketamine/xylazine
125 cocktail (80 mg/kg and 10 mg/kg, respectively). The absence of eye-blink and paw-
126 withdrawal reflexes was ensured prior to proceeding. Anesthetized animals were then
127 placed on a platform beneath an open-ended shock tube to be exposed to the blast
128 event, as described in our prior publications (Song et al. 2015; Walls et al. 2016; Race et
129 al. 2017).
130
131 For the Blast group, each rat's head was positioned beneath the open end of the shock
132 tube such that the dorsum of the skull was the incident surface exposed to a composite
133 blast (shock wave + blast wind). A custom plexiglass housing was temporarily placed over
134 the animal's torso for body protection to avoid cardiac or pulmonary effects of blast and
135 to simulate the protective effects of military body armor (Rafaels et al. 2011). The head
136 was fixed with a stereotaxic head frame with bite bar and ear bars (Kopf Instruments) to
137 prevent blast wind-induced head acceleration. The blast exposure exhibited a recorded
138 pressure profile with a rise to peak pressure within 0.3 msec, followed by overpressure
139 and underpressure periods as follows: side-on (static) 150 kPa maximum overpressure,
140 1.25 msec overpressure duration, and 20 kPa minimum underpressure; face on (dynamic)
141 160 kPa maximum overpressure, 1.75 msec overpressure duration, and 5 kPa minimum

142 underpressure. These conditions were the same as reported in our prior publications
143 (Song et al. 2015; Walls et al. 2016; Race et al. 2017). All but one blast animal survived the
144 exposure without displaying any external deficit during each animal's longitudinal follow-
145 up period.
146
147 Sham animals were placed equidistant from the blast source, but out of the path of the
148 shockwave, therefore only exposed to the blast noise. Tympanic membrane integrity was
149 verified for all Blast and Sham animals after injury using a surgical microscope.
150 *(Insert Fig. 1 about here)*
151
152 Auditory Evoked Potential Recordings
153 The animals underwent two-channel Auditory Evoked Potential (AEP) recordings at the
154 following time points: pre-exposure (baseline), 1 day, 4 days, 7 days, 10 days, 14 days, 1
155 month, and 2 months. While the animals were under 1.8-2% isoflurane anesthesia,
156 subdermal needle electrodes (Ambu) were inserted in the following locations (Fig. 1A):
157 Channel 1 positive electrode was placed along the midline of the head (mid-sagittal)
158 oriented Fz to Cz. Channel 2 positive electrode was positioned C3 to C4 along the
159 interaural line. The negative/inverting electrode (used with positive electrodes for both
160 channels 1 and 2) was placed under the mastoid of the right ear ipsilateral to the speaker.
161 A ground electrode was placed in the back of the animal. These configurations were
162 consistent with prior publications from our laboratory (Parthasarathy and Bartlett 2011,
163 2012; Parthasarathy et al. 2014; Lai and Bartlett 2015; Lai et al. 2017). Electrode

164 impedances were confirmed to be less than 1 kΩ using a low impedance amplifier (RA4LI,
165 TDT). After electrode placement, we subsequently sedated the animals by intramuscular
166 injection of 0.2-0.3 mg/kg dexmedetomidine (Dexdomitor). AEP recordings were
167 performed 10-15 min after removal from isoflurane to avoid anesthetic effects. The
168 animals could respond to pain and acoustic stimuli but tend sit calmly under
169 dexmedetomidine sedation, allowing about 3 hours of recording time.
170
171 Acoustic stimuli were presented free-field to the right ear (90° azimuth) of animals, with
172 directly in front of the animals' face as the reference for 0° azimuth, using a calibrated
173 speaker (Bowers and Wilkins) at a distance of 115 cm directly facing the right ear. The
174 measurements used in this study included auditory brainstem responses (ABRs), middle-
175 latency responses (MLRs), envelop-following responses (EFRs) using AM in noise stimuli,
176 and IRNs.
177
178 ABR and MLR
179 6 Sham animals and 10 Blast animals were used in ABR analysis. For ABR, rectangular
180 clicks (0.1 msec duration) and tone-pips (2 msec duration, 0.5 msec $\cos^2$ rise-fall time)
181 with frequencies of 8 kHz and 16kHz were used. 8 kHz and 16 kHz were chosen based
182 on previous findings: with 6-16 kHz being the most sensitive hearing region of rats, 8 kHz
183 near the most sensitive region of normal rat audiogram (Parthasarathy et al. 2014) and
184 hearing of frequencies higher than 8 kHz being most vulnerable to blast injury (Race et
185 al. 2017). The sound levels of clicks and pips ranged from 90 to 10 dB peak SPL in 5-dB

steps. All stimuli were presented in alternating polarity at 26.6 per second with 1500 repetitions (750 at each polarity). A 20 msec acquisition window (0-20 msec) was used. Data were processed with a 30 Hz high-pass (HP) filter and a 3000 Hz low-pass (LP) filter prior to analysis. The ABR threshold was visually determined as the minimum sound level that produced a distinct ABR waveform, with confirmation from two other researchers. The ABR amplitudes of waves I and V from channel 2 were estimated as the differences of each wave's amplitude, as seen in BioSigRP (TDT) and the baseline amplitude (measured as an average of 2 msec waveform prior to the cochlear microphonic).

6 Sham animals and 8 Blast animals were used in MLR analysis. For MLR, similar rectangular clicks and 8 kHz tone pips of alternating polarity as in ABR were used but were presented at a slower rate (3.33/sec vs. 26.6/sec in ABRs) and with a recording window of longer duration (100 msec vs. 20 msec in ABRs). This time window provides enough time to capture the stimulus-evoked "middle-latency" neural responses from the auditory midbrain, thalamus and cortex (Barth and Shi Di 1991; McGee et al. 1991; Di and Barth 1992; McGee and Kraus 1996; Phillips et al. 2011; Šuta et al. 2011) alongside ABR. Stimuli were presented at 80 dB sound pressure level (SPL) and 30 dB sensation level (SL, 30 dB above corresponding ABR thresholds), as determined in the previous ABR recordings. 1500 repetitions were collected over an acquisition time window of 100 msec to obtain an average response. Only one animal exhibited hearing threshold higher than 80 dB SPL at only one time point, for which MLR recording has been excluded for that point.

208 Data were processed with HP (fc = 10 Hz) and LP (fc = 300 Hz) filters prior to analysis.

209

210 **EFRs**

211 EFRs were recorded during the same recording session following ABRs and MLRs using
212 the same electrode configurations with similar techniques to Lai and Bartlett (2018) and
213 Lai (Lai et al. 2017). The two channels were sensitive to a complementary range of
214 amplitude modulation frequencies (AMFs) (Parthasarathy and Bartlett 2012), with channel
215 1 (mid-sagittal) being more sensitive to higher AMFs (90-2048 Hz) while channel 2
216 (interaural) is more sensitive to lower AMFs (8-90 Hz). The AM stimuli used for EFRs were
217 sinusoidally amplitude-modulated (AM) sounds, with Gaussian noise, 8 kHz tone, or 16
218 kHz tone as carriers, and under 100% and 50% modulation depth with a stimulus duration
219 of 200 msec. The AMFs selected for this study are 10 Hz, 45 Hz, and 256 Hz, based on
220 the findings in Race at al. (Race et al. 2017), which found significant differences,
221 particularly at the lower AMFs. The acquisition window was 300 msec long, and each
222 response was an average of 200 repetitions. The stimuli were presented at 30 dB SL. For
223 animals that had a hearing threshold above 70 dB SPL, which usually happens on day 1
224 post-exposure, EFR was not collected at the time point due to the limitation of the
225 speaker and BiosigRP.

226

227 For AM in Noise stimuli, the same EFRs were used alongside a 71 Hz sinusoidally AM
228 masker of the same length and onset, with Gaussian noise as the carrier, similar to Lai
229 and Bartlett (Lai and Bartlett 2018). Noise AM maskers were presented at sound levels of

20dB SNR and 0SNR to the sound level of target AM. Prior to EFR amplitude analysis, data were passed through an LP filter of 3000 Hz and a high-pass filter that was either slightly below the AMF for AMFs <90 Hz, or 80 Hz for AMFs ≥ 90 Hz.

IRNs

For 6 Sham animals and 8 Blast animals, IRNs were recorded during the same recording session following the previous stimuli using the same electrode configurations. The sound level of presentation was 30 dB SL (above click hearing threshold). Data for animals with a hearing threshold above 70 dB SPL were not collected at the time point.

IRN tone stimuli were created by sequential delay and add operations. Time-varying pitch curves were created by applying polynomial equations to create delays constructed from the fundamental frequencies of Chinese tone 2 and tone 4, delaying Gaussian noise (80 Hz-40 kHz) by the inversion of pitch and adding it back on itself in a recursive manner (Yost 1996a). The core MATLAB program used for generating IRN was modified from Krishnan et al. (Krishnan et al. 2014, 2015) This would generate dynamic, curvilinear pitch patterns (Swaminathan et al. 2008) that preserves variations in pitch using a broadband carrier. The number of iteration steps for these stimuli was 32, beyond which there is little or no change in pitch salience (Yost 1996b).

IRN iteration (ite) stimuli were created with the same polynomial equations used for tone 2, but with different iterations to create an array of IRN stimuli with different pitch salience.

The numbers of iteration steps were 32, 16, 8, 4, and 2.

All IRN stimuli consisted of pairs of waveforms in original and inversed polarities to compensate for envelope or fine structure response under different calculations and cancel any microphonics. The stimulus duration was 250 msec, and the acquisition window was 300 msec long. Each response was an average of 200 repetitions.

Statistics

Statistics were performed with statistics software JASP (Version 0.11, JASP Team, 2019). All statistics for ABR and EFR utilized 2-way repeated measures ANOVA test ($\alpha = 0.05$) to check the significance of each main effect and interaction, undergoing Greenhouse-Geisser sphericity corrections (Greenhouse and Geisser 1959) and Tukey Post Hoc corrections (Tukey 1949). For ABR statistics, Wave I (channel 2), III (channel 1) and V (channel 2) were measured at each time point (Fig. 1B), corresponding to the auditory nerve (Wave I), cochlear nucleus (Wave III), and rostral brainstem/IC sources (Wave V) (Parthasarathy and Bartlett 2012; Simpson and Prendergast 2013). For EFR statistics, responses were analyzed from channel 2 for 10 Hz and 45 Hz, and from channel 1 for 256 Hz (Parthasarathy and Bartlett 2012). Prior to statistical tests, EFR amplitudes at signal frequencies were acquired through Fast Fourier Transformation (FFT) in MATLAB (MathWorks) similar to (Lai and Bartlett 2018).

For MLR statistics, P1, N1, P2, and N2 (Fig. 5A) peaks were measured at each time point, corresponding to subcortical (P1), thalamocortical (N1) and cortical sources (P2, N2)

(Simpson and Prendergast 2013). Peak amplitudes were normalized to the pre-blast exposure baseline measurements for display in Fig. 5C, D. The peak amplitudes at each time point were compared to the pre-stimulus baseline using a paired sign-rank test, with a 0.05 significance criterion.

For IRN statistics, we performed moving-window autocorrelations in 25 msec moving windows (5 msec steps) on each response waveform to simulate physiological tracking of temporal periodicity. Peak autocorrelation frequency was defined by the inverse of the time lag where peak autocorrelation value occurs in each window. This process yielded a total of 51 peak frequencies that reflect the frequency representation of the IRN auditory response. Of those, 45 occurred during the stimulus. The peak frequencies were then compared to the "pseudopitches" of the IRN stimuli on corresponding time points. A value within 5 Hz of absolute difference to corresponding "pseudopitch" was considered "tracked." We used this number of "tracked" peak frequencies, or "pitch-tracking score," as a quantification for IRN performance. The significance of each main effect (time, blast condition, and IRN iterations) and interaction was assessed using similar 2-way repeated measures ANOVA test as ABR statistics ($\alpha = 0.05$). For response-to-response correlation (Fig. 8D), the cross-correlation was measured between the response to the IRN stimuli pre-exposure and the response to the same stimulus post-exposure. Blast versus sham group was tested using the paired sign-rank test for this measure ($\alpha = 0.05$).

Results

296 A. ABR and MLR

297 ABR Thresholds

298 *(Insert Fig. 2 about here)*

299 Click ABR recordings captured distinctive courses of threshold changes over the two
300 months post-exposure for blast and sham animals (Fig. 2). A large, >30dB SPL maximum
301 threshold increase was observed in post-blast-exposure animals (Fig. 2, red lines).
302 Adjacent animals exposed only to blast noise (Sham) did not undergo significant
303 threshold shifts (Fig. 2, blue lines). Thresholds for blast group animals showed clear
304 recovery during the first two weeks, with the largest changes occurring between 4 days –
305 10 days. Thresholds for blast-exposed animals remained significantly elevated (worse)
306 than those of sham animals throughout the two months post-exposure that were
307 measured ($F=12.727$, $p=0.003$). Significant main effects of both Group ($F=61.943$,
308 $p=<0.001$, $\eta^2_p=0.816$) and Time Point ($F=41.932$, $p<0.001$, $\eta^2_p=0.750$), as well as a
309 significant Group*Time Point interaction effect ($F=23.503$, $p<0.001$, $\eta^2_p=0.627$), were
310 observed.

311

312 Similar trends were observed with tone ABR recordings of 8 kHz and 16 kHz (Fig. 2), with
313 a significant ($p\leqslant0.001$) >30 dB increase in threshold within 48 hours post-blast-exposure
314 and most prominent recovery between 4 days – 10 days. 8 kHz threshold differences
315 between blast conditions became non-significant ($F=3.151$, $p=0.098$) at 10 days post-
316 blast. At two weeks post-exposure, 16 kHz thresholds remained significantly elevated
317 ($F=16.527$, $p<0.001$), after which point the thresholds for the two chosen tone frequencies

were no longer significantly different between Blast and Sham. Our rmANOVA analysis using Group and Time Points as factors showed significant main effects of Group (8 kHz: $F=10.847$, $p=0.005$, $\eta^2_p=0.437$; 16 kHz: $F=19.697$, $p<0.001$, $\eta^2_p=0.585$), Time (8 kHz: $F=25.837$, $p<0.001$, $\eta^2_p=0.649$; 16 kHz: $F=20.181$, $p<0.001$, $\eta^2_p=0.590$) and Group*Time Point interaction (8 kHz: $F=13.490$, $p<0.001$, $\eta^2_p=0.491$; 16 kHz: $F=15.860$, $p<0.001$, $\eta^2_p=0.531$) for 8 kHz and 16 kHz threshold respectively. These results demonstrate that broadband click thresholds remain significantly elevated over the 60 days measurement window. 8 kHz thresholds largely returned to baseline (Day 30: 8 dB difference, $p=0.118$; day 60: 4 dB difference, $p=0.965$) after two weeks, and 16 kHz thresholds remained significantly elevated compared to pre-blast baseline according to post hoc analysis (Day 30: 15.5 dB difference, $p<0.001$; day 60: 14.5 dB difference, $p<0.001$), although the difference between blast and Sham was not significant at these time points.

ABR Amplitudes

(Insert Fig. 3 about here)

For our ABR and MLR measurements, we used two sound levels: 80 dB SPL was chosen because it is commonly used in auditory evoked potential studies in rat and human studies (Simpson et al. 1985; Alvarado et al. 2012; Race et al. 2017), and it elicits clear ABR responses in all except the most extreme cases of blast-exposure. In order to compensate for changes in threshold induced by blast exposure, we also measured ABR amplitudes at 30 dB SL above threshold (sensation level, or SL). This enabled us to separate changes in ABR amplitudes due to audibility (threshold) versus those due to threshold-

independent changes in subcortical auditory signaling. Note that we did not attempt to compare later ABR waves with equivalent wave I amplitudes, as in Lai et al. (2017).

ABR wave amplitudes were assessed for wave I (putative auditory nerve), III (putative cochlear nuclei), and V (putative rostral brainstem and inferior colliculus) in response to click stimuli at 80 dB SPL (Fig. 3) and 30 dB SL (Fig. 4). Repeated measures statistics for 80 dB SPL and 30dB SL are shown in Tables 1-4.

Wave I: Wave I amplitudes at 80 dB SPL for all ABR carriers at 80 dB SPL exhibited significant main effects of Group, Time, and Group*Time interaction (Table 1). Compared to pre-exposure responses, wave I amplitudes were significantly smaller at all time points tested in blast animals for clicks, 8 kHz tones, and 16 kHz tones, indicating lasting cochlear/auditory nerve damage (Table 4). No significant changes in wave I amplitudes were observed in Sham exposed animals at any time point.

Wave III: Wave III amplitudes at 80 dB SPL for all ABR carriers at 80 dB SPL exhibited significant main effects of Group, Time, and Group*Time interaction (Table 1), with Group effects lasting for 14 days for Click and 16 kHz tones and 10 days for 8 kHz tones. Compared to pre-exposure responses, wave III amplitudes were significantly smaller at all time points tested in blast animals for clicks and 16 kHz tones and up to 30 days for 8 kHz tones, indicating lasting declines in cochlear nucleus excitation (Supplemental Materials). No significant changes in wave III amplitudes were observed in Sham exposed animals at any time point.

Wave V: Wave V amplitudes at 80 dB SPL for all ABR carriers at 80 dB SPL exhibited

362 significant main effects of Group, Time, and Group*Time interaction (Table 1), with Group
363 effects lasting for 14 days for Click and 16 kHz tones and 7 days for 8 kHz tones.
364 Compared to pre-exposure responses, wave V amplitudes were significantly smaller at all
365 time points tested in blast animals for clicks, indicating lasting declines in rostral
366 brainstem/IC excitation for brief, broadband clicks (Table 4). However, decreases in wave
367 V amplitudes persisted for only 7 days for 8 kHz tones and 14 days for 16 kHz tones,
368 suggesting that despite decreases in cochlear nucleus excitation (as represented by wave
369 III amplitude), rostral brainstem/IC responses compensated and restored their responses.
370 No significant changes in wave V amplitudes were observed in Sham exposed animals at
371 any time point except for a small decline for 16 kHz responses 60 days post Sham
372 exposure (Table 4).
373
374 *(Insert Fig. 4 about here)*
375
376 The effects on ABR waves were greatly diminished when responses to 30 dB SL sounds
377 were measured, as shown in Table 2 and Table 3. For Wave I, significant main effects of
378 Time (Click: $F=2.554$, $p=0.043$, $\eta^2_p=0.154$; 8 kHz: $F=3.146$, $p=0.018$, $\eta^2_p=0.183$; 16kHz:
379 $F=2.325$, $p=0.031$, $\eta^2_p=0.142$) but not Group (Click: $F=3.637$, $p=0.077$, $\eta^2_p=0.206$; 8 kHz:
380 $F<0.001$, $p=0.994$, $\eta^2_p<0.001$; 16kHz: $F=1.046$, $p=0.324$, $\eta^2_p=0.070$) were observed for
381 click, 8 kHz, and 16 kHz. Additionally, significant Group*Time interaction effects were only
382 observed for Click ($F=2.630$, $p=0.039$, $\eta^2_p=0.158$) and 16 kHz ($F=2.381$, $p=0.027$, η^2
383 $_p=0.145$). Simple main effects of Group were only observed in Click (Table 3).

384 Compared to pre-exposure responses, wave I and V responses to clicks were significantly
385 reduced 1 day post-blast and wave III responses were significantly reduced days 1-4.
386 Otherwise, there were no significant declines in wave amplitudes in the Blast group, and
387 there were no significant amplitude changes in the Sham group.
388
389 *(Insert Fig. 5 about here)*
390
391 B. MLR

392 In order to observe thalamocortical and cortical neural transmission in response to
393 acoustic transients, we recorded middle-latency auditory responses to click and 8 kHz
394 tone stimuli. These stimuli were identical to those used for ABR, but the presentation rate
395 was much slower, and the analysis window and filters were different (see Methods).
396 Measurements were made for the first four main peaks of the MLR. Here, P1 corresponds
397 to subcortical activity, largely encompassing the ABR. N1 corresponds to thalamocortical
398 transmission, while P2 and N2 are thought to correspond to primarily cortical activity
399 (Deiber et al. 1988; Liégeois-Chauvel et al. 1994; Tichko and Skoe 2017; Musiek and Nagle
400 2018).
401
402 80 dB SPL responses
403 In blast animals, all waves were decreased relative to pre-blast baseline for days 1-7 post-
404 blast ($p<0.05$, sign-rank test) in response to 80 dB SPL click stimuli. Grand average traces
405 are shown for MLR responses in this time window in Fig. 5A, relative to the pre-blast

406 waveform (thick blue line in A-D). Even after the blast, the morphology and timing of the
407 MLR waveform remained relatively intact, but the amplitudes were significantly
408 diminished. In Fig. 5E-H, wave amplitudes were normalized to the pre-blast waves and
409 measured. Between 7 and 10 days, the early P1 wave recovers to within 10-15% of its
410 baseline amplitude, whereas the later waves recovered more slowly (Fig. 5E). In particular,
411 the N1 wave, thought to reflect thalamocortical transmission (Barth and Shi Di 1991;
412 McGee et al. 1991, 1992; Di and Barth 1992; Brett et al. 1996; McGee and Kraus 1996;
413 Phillips et al. 2011; Šuta et al. 2011), remained significantly lower in blast animals even 60
414 days post-blast ($p<0.05$, sign-rank test, Fig. 5E). By contrast, the MLR waves in sham
415 animals were largely stable across the measurement time (Fig. 5F). Although there was
416 some decline in the later waves for the last time window, this was not statistically
417 significant (Fig. 5B, D, F).
418
419 MLR responses to 8 kHz, 80 dB SPL tone pips largely mirrored the results to clicks, with
420 significant decreases for all waves for post-blast days 1-7 and a lasting decline in N1 for
421 the duration of measurements ($p<0.05$, sign-rank test, traces not shown). Sham
422 responses did not show any significant changes in MLR waves in response to the 80 dB
423 SPL tone pips.
424
425 30 dB SL
426 MLR responses to clicks at 30 dB SL were reduced in Blast animals 1 day after the blast
427 but recovered to baseline levels afterwards. There was a tendency towards elevated P1

428 amplitudes, but this was not significant (Fig. 5G). Sham animals did not show any
429 significant changes, though there was a tendency towards an increase in wave amplitude
430 (Fig. 5H). Similar results were found for responses to tones at 30 dB SL (not shown).
431

432 ### C. EFR and EFR in noise

433 Given the different time courses and extents of ABR threshold change for clicks and tones,
434 we measured the corresponding EFRs in response to Gaussian broadband noise (NAM),
435 8 kHz, and 16 kHz sinusoidal tone carriers. Considering that slow AM (<50 Hz) and faster
436 AM (>50 Hz) are differentially represented throughout cortical and subcortical auditory
437 nuclei (Joris et al. 2004; Wang et al. 2008), three representative AMFs (10, 45, and 256 Hz)
438 were selected from previous publications (Parthasarathy et al. 2010, 2014; Parthasarathy
439 and Bartlett 2011, 2012; Race et al. 2017) and tested in quiet at 100% and 50% modulation
440 depth. AM stimuli were also presented at 30 dB SL with a 71 Hz sinusoidally AM masker
441 of the same length and onset, with Gaussian noise as the carrier, at 20dB SNR and 0 SNR
442 relative to the sound level of target AM. For each carrier, simple main effects of all
443 conditions were analyzed.
444 *(Insert Fig. 6 about here)*
445

446 **EFRs in quiet:** For all three carriers in quiet, EFR amplitudes were similar at 10 and 256 Hz
447 across time points and AM modulation depths (Fig. 6). Overall, the NAM FFT amplitudes
448 were reduced in the Blast group in quiet ($F=9.629$, $p=0.0018$, $\eta^2_p=0.426$), with 45 Hz
449 being the most affected. Interestingly, in contrast to the lower FFT Amplitude found in

Blast AM at 80 dB SPL (Race et al. 2017), when the hearing threshold has been compensated, FFT amplitude of 45 Hz NAM was higher in Blast than in Sham animals. This difference was most salient on day 7 for 45 Hz NAM ($p=0.006$). For 8 kHz SAM and 16 kHz SAM, the slight elevation of AM FFT Amplitude in Blast animals was not significant. Surprisingly, time did not have a significant interaction across repeated measures for AM response with any carrier either.

EFR in noise: Not surprisingly, Noise level and Modulation Depth both had a significant repeated measures effect on NAM (Noise level: $F=263.217$, $p<0.001$, $\eta^2_p=0.953$; Depth: $F=455.655$, $p<0.001$, $\eta^2_p=0.972$), 8 kHz SAM (Noise level: $F=19.308$, $p<0.001$, $\eta^2_p=0.580$; Depth: $F=72.031$, $p<0.001$, $\eta^2_p=0.837$) and 16 kHz SAM (Noise level: $F=16.691$, $p<0.001$, $\eta^2_p=0.544$; Depth: $F=49.742$, $p<0.001$, $\eta^2_p=0.780$). Noise level and Depth also have a significant interaction effect with Blast Groups for NAM overall (Noise level: $F=10.295$, $p<0.001$, $\eta^2_p=0.442$; Depth: $F=6.057$, $p=0.029$, $\eta^2_p=0.318$), showing blast NAM responses as less affected 20 SNR noise, but more sensitive amplitude declines for lower modulation depth. Noise level also affects 8 kHz SAM differently between Groups ($F=5.696$, $p=0.008$, $\eta^2_p=0.289$). These conditions do not have significant interaction effects with Blast Group on 16 kHz SAM. Noise level had significant interaction effects with both Blast Group ($F=6.130$, $p=0.011$, $\eta^2_p=0.320$) and Depth ($F=19.438$, $p <0.001$, $\eta^2_p=0.599$) for NAM 45 Hz, while the effect of Time or Depth between Groups is not significantly different for any modulation frequency.

(Insert Fig. 7 about here)

For 8 kHz SAM, the effects of Noise level were applied differently between Blast Groups, as significant interaction effects were observed between Noise and Group for 10 Hz ($F=12.795$, $p=0.001$, $\eta^2_p=0.477$) and 45 Hz ($F=4.878$, $p=0.015$, $\eta^2_p=0.258$) modulation frequencies, though not for 256 Hz. Modulation Depth affects FFT amplitude without regard to blast condition, with no significant interaction effects with Group observed. For 16 kHz SAM, none of the parameters tested had significantly different effects between Groups at 30 dB SL (not shown).

D. IRN

Time-varying IRN stimuli were used to elicit frequency-following response (FFR) mimicking Mandarin tone 2 (T2, rising) and tone 4 (T4, falling) pitch contours to measure pitch-tracking ability using a broadband speech-like carrier at 30 dB SL, similar to what has been measured in human studies of auditory learning and hearing loss (Anderson et al. 2010, 2013; Skoe and Kraus 2010). We used autocorrelation interval contours that simulated pitches similar to the forms of rising (T2) and falling (T4) pitch contours of the Mandarin Chinese vowel /yi/ (Krishnan et al. 2014, 2015, 2017a, 2017b). IRN responses were evaluated based on the pitch-tracking score, which measures the number of windows where the dominant autocorrelation frequency of the response matches that of the IRN stimulus autocorrelation frequency (see Methods). In general, we observed a loss of pitch-tracking fidelity in Blast animals over the two months post-exposure. Even for

494 the most salient pitch (32 Iterations), blast exposure had a significant Group effect on
495 pitch-tracking scores in both Tone 2 ($F=6.495$, $p=0.026$, $\eta^2_p=0.351$) and Tone 4 ($F=6.115$,
496 $p=0.029$, $\eta^2_p=0.338$), with the largest mean differences on day 7-10. The interaction
497 effect between Time and Group was not significant.
498 Blast exposure significantly changed the neural response's morphology to IRN at 30 dB
499 SL ($p=0.016$, paired sign-rank test, Fig. 8D), such that the cross-correlation between the
500 pre-exposure response and the post-exposure response was much lower in the Blast
501 group up to 30 days post-blast.
502 *(Insert Fig. 8 about here)*
503
504 **IRN iterations:** As expected, reduced pitch salience, controlled by reducing iteration
505 number, affected pitch-tracking responses in animals ($F=41.697$, $p<0.001$, $\eta^2_p=0.777$),
506 also showing a significant interaction effect with Time post-exposure ($F=1.722$, $p=0.031$,
507 $\eta^2_p=0.125$). Specifically, pitch-tracking performances to 32 iterations and 16 iterations
508 worsened significantly up to 7-10 days post-exposure, with various degrees of recovery
509 over the following time course. Both the Blast and Sham group exhibited worse pitch
510 tracking with reduced iterations (salience) and to a similar degree. No significant
511 interaction effects with Group were observed for Time and Iterations (Fig 9).
512 *(Insert Fig. 9 about here)*
513
514 ## Discussion
515 The purpose of this study was to examine the time course of recovery from a single mild

516 blast injury using simple and complex auditory stimuli longitudinally over a two-month
517 period. Our study demonstrated drastic changes in high-frequency and click hearing
518 thresholds from ABR recordings and reductions in putative subcortical and
519 thalamocortical transmission from ABR and MLR recordings throughout the first two
520 weeks post-exposure. At 30-60 days post-blast, significant increases in click threshold,
521 decreases in wave I amplitude, decreases in MLR N1 amplitude, and declines in pitch-
522 tracking of speech-like IRN pitch trajectories were observed. Compensating for threshold
523 shift and using 30 dB sensation level for AM stimuli, we found that responses to sinusoidal
524 AM stimuli in quiet or noise recovered within 14 days. The 7-14 day window was
525 particularly rapid in the recovery of many auditory parameters, suggesting this as a
526 therapeutic time period when important changes take place.
527
528 ABR
529 We documented the rapid increase of threshold and slow recovery after trauma from
530 blast-exposure. Most notably, a >30 dB peak increase in threshold was observed for
531 click, 8 kHz, and 16 kHz (Fig. 2) during the first 4 days. This is consistent with the
532 description of IHC and OHC disturbances across a wide range of frequencies due to
533 blast overpressure as stated in multiple previous publications (Patterson and Hamernik
534 1997; Ewert et al. 2012; Race et al. 2017). Cho et al. (2013b) reported that ABRs exhibit
535 the least recovery at the highest and lowest frequencies. This broadband threshold shift
536 extended to the last time point at 60 days, though the ~10 dB difference would not be
537 considered clinically relevant.

538 Over the two-month observation, rapid improvements in ABR threshold and wave
539 amplitudes were observed in the 7-10 days recovery period for waves I, wave III, and
540 wave V (Fig. 3). Such rapid recovery could be explained by neuroplastic remodeling within
541 central auditory ABR generator regions (Mulders and Robertson 2009, 2011, 2013;
542 Mulders et al. 2011; Manzoor et al. 2013; Robertson et al. 2013) and recovery of hearing
543 thresholds. Notably, wave V amplitude recovered earlier than wave I, possibly indicating
544 the role of compensation in auditory midbrain as one of the post-blast recovery
545 mechanisms.
546
547 We hypothesized that the recovery of ABR threshold and wave I amplitude were the
548 results of a two-fold process, with persistent changes contributing to degraded speech
549 perception (Holmes and Griffiths 2019; Yeend et al. 2019). These parameters showed two
550 waves of post-blast changes: one between 1-10 days post-exposure, and one 10-30
551 days, as evidenced by Figs. 2 and 3. We hypothesize that these two waves of deficits
552 indicated the distinction of primary, physical impacts to multiple loci in PAS and CAS
553 (Garman et al. 2011; Ewert et al. 2012; Cho et al. 2013b; Song et al. 2015; Walls et al. 2016)
554 and a series of secondary, biochemical impacts surrounding CAS (Laplaca et al. 1997;
555 Knudsen and Øen 2003; Hamann et al. 2008; Garman et al. 2011; Säljö et al. 2011; Luo et
556 al. 2014a, 2014b; Song et al. 2015; Walls et al. 2016). Our observations of blast recovery
557 were mostly consistent with this hypothesis.
558
559 MLR

560 At 80 dB SPL, we found persistent deficits in thalamocortical and cortical transmission
561 based on the N1, P2 and N2 peaks (Fig. 5A vs. B, C vs. D), which were affected at 30 and
562 60 days, even after the early P1 response had fully recovered (Fig 5E). These deficits were
563 not present at 30 dB SL, suggesting that effects were at least partially due to shifts in
564 auditory thresholds (Fig. 5G), but the moderate, subclinical threshold shifts observed are
565 probably highly relevant functionally. In veterans and the general population with lifetime
566 noise exposure, MLR responses were shown to be smaller even when subjects had
567 clinically normal audiograms, and there was some evidence of increased cortical gain
568 (Valderrama et al. 2018; Bramhall et al. 2020). In another study with blast-exposed
569 veterans, most of the changes in auditory-evoked potentials were correlated with hearing
570 loss (Meehan et al. 2019). Together, these results suggest that hearing loss may be the
571 main contributor to MLR changes leading to declines in suprathreshold responses.
572 However, more work needs to be done for sustained sounds post-blast to examine the
573 relationships between early evoked potentials, representing subcortical neural activities,
574 and later potentials, representing cortical activities, since studies in aging and noise
575 exposure have suggested enhanced cortical responses (Syka and Rybalko 2000; Sun et al.
576 2012; Bidelman et al. 2014; Herrmann et al. 2019). These results also suggest that there
577 may be more pronounced hearing deficits from intense combined auditory and
578 mechanical trauma such as blast, compared to medium to intense level of auditory
579 exposure alone, such as recreational or occupational noise (Fulbright et al. 2017; Grinn et
580 al. 2017; Guest et al. 2018).
581

582 Amplitude Modulation EFRs

583 The current study extended an earlier study (Race et al. 2017) to include EFR responses
584 to more challenging auditory stimuli, including lower modulation depth (Fig 6) and in the
585 presence of modulated noise (Fig 7). The Race et al. (2017) study revealed differences in
586 AM processing at 80 dB SPL between Blast and Sham animals, such that blast animals
587 had lower AM FFR amplitudes, especially at lower modulation frequencies in the 20-50
588 Hz range. However, when the hearing threshold has been compensated, the differences
589 in AM FFR amplitude diminished and even changed sign (Fig. 6), suggesting that both
590 changes in audibility and changes in the gain of subcortical auditory system are critical
591 contributors to AM FFR deficits in the blast-exposed auditory system. There are
592 complicated interactions between the AM FFR amplitudes, blast exposure, and the
593 presence of noise, evident as a persistent Group*Noise Level interaction effect in both
594 NAM and 8 kHz SAM. AM responses consist of contributions from multiple generators
595 along the auditory neuraxis, with cortical generators contributing mainly to lower AMFs
596 <50 Hz, and higher frequency AM responses limited to nuclei lower in the auditory
597 neuraxis. The lack of blast-induced differences at higher AMFs distinguishes the blast-
598 induced damage from age-related changes, which are most prominent at higher
599 modulation frequencies (Parthasarathy et al. 2010, Parthasarathy and Bartlett 2012, Lai et
600 al. 2017).

601

602 The differences in low-middle AMFs were manifested in opposed directions under slow
603 (10 Hz) and middle (45 Hz) AMFs: notably, normalized FFT amplitudes of 8 kHz SAM in

604 noise is lower for Blast at 10 Hz modulation frequency, but higher for Blast at 45 Hz (Fig
605 7D). This dichotomy is ripe for further study since the 10 Hz and 45 Hz modulations
606 represent different temporal processing regimes and components of speech (Rosen
607 1992). In studies on age-related auditory nerve deficit models and AM-in-noise
608 responses in aged animals, decreased sensitivities to lower SNRs in AM-in-noise in
609 damaged auditory systems have been observed (Parthasarathy et al. 2016; Lai et al. 2017;
610 Lai and Bartlett 2018). This phenomenon could partly explain the changes seen in 45 Hz
611 AMF. It should be noted that the variance in AM responses post-blast exposure could
612 also be a result of post-blast increases in spontaneous activity for DCN and IC units
613 sensitive to tone versus noise carriers (Luo et al. 2014a, 2014b), which could either
614 desynchronize responses or strengthen AM response simply by heightened excitability.
615
616 Taken together, our results suggested that: 1) CAS neuroplasticity partially compensates
617 for hearing loss after blast exposure; and 2) surprisingly, at least for a single mild blast
618 with small lasting threshold shifts, our results suggest that sinusoidal AM processing in
619 quiet and noise largely recovers.
620
621 IRN EFRs
622 Bressler et al. (2017) have noted that perceptual and behavioral deficits persist in blast-
623 exposed veterans in the absence of major clinical threshold or ABR abnormalities.
624 Simple auditory tests such as ABRs and AM EFRs in a quiet background are limited
625 indicators of auditory challenges that blast-exposed individuals would face in daily life.

The present study investigated how noise affects responses post-blast as well as using IRN stimuli that simulate the pitch trajectories and sound like simple speech sounds. These stimuli may capture the more complex hearing deficits reported by humans who have experienced blast injuries (Gallun et al. 2012a; Saunders et al. 2015; Kubli et al. 2018).

Complex temporal periodicity between 50 Hz and 500 Hz carries important speech information such as voicing, stress and intonation (Rosen 1992). The present study provided insights into blast-induced sound processing deficits through the use of an IRN stimulus that simulates Chinese intonations and whose pitch and salience can be reliably controlled, showing that IRN can be a useful diagnostic tool for neurotrauma. We found out that even when click ABR thresholds have returned to subclinical threshold shifts, the deficits in pitch-tracking response to IRN tone stimuli, lingered at least 30 days post-exposure (Figs. 8D).

Decreased salience (fewer iterations), showed an overall reduction in pitch tracking in Blast animals (Fig. 9), particularly for higher iterations which should be most salient, but they were not differentially affected by the number of iterations. It is worth noting that a previous study showed that increased IRN iterations improved auditory stream segregation in normal hearing veterans more than hearing-impaired veterans (Shearer et al. 2018). Our IRN data (Figs. 8-9) suggest that more dynamic and speech-like modulation changes do not recover quickly or completely from even a single mild blast exposure.

Limitations and Future Directions

This study has examined injuries elicited by a single dorsal blast exposure with body shielding that did not result in tympanic membrane ruptures. Therefore, the deficits observed may not be as drastic as that documented by some previous studies in which the injuries were caused by more intense or multiple exposures (Cho et al. 2013b; Du et al. 2013; Luo et al. 2014a, 2014b; Mahmood et al. 2014), often resulting in death or tympanic membrane rupture. The distribution of injuries also differed from models in which blast exposure comes from different orientations, as predicted in animals (Chavko et al. 2011; Dal Cengio Leonardi et al. 2012) and computational studies (Hua et al. 2017; Unnikrishnan et al. 2019). These differences in pressure wave amplitude, duration, and propagation patterns would affect both the distribution and severity of damage across the brain. Although these could change the potential mechanisms of recovery and compensation, it is likely that all blast exposures undergo a multi-stage recovery process similar to that observed in the present study. Our model utilized a top-down mild blast model as described by Song et al. (2015), which exerts a blast impact from the top of the skull. The overpressure blast wave passes through the entire rat brain, such that TBI can be observed throughout the brain, including the frontal cortex and in multiple thalamic regions (Walls et al. 2016), and it results in increased ventral BBB membrane permeation and inflammation, encompassing many subcortical auditory nuclei and axonal tracts. While overlapping loci of vulnerability were described in anatomical studies of animal exposed to blast impacts of different or unknown orientations (Knudsen and Øen 2003; Säljö et al. 2011; Mao et al. 2012b), additional injury mechanisms of different loci and

670 nature may be expected from blast impacts from a different angle. Moreover, non-
671 invasive physiological measurements of the auditory thalamus and cortex may be
672 indicators of more widespread blast damage in auditory and non-auditory brain regions.
673

674 ## Conclusion

675 Based on our chronic longitudinal AEP measurements over a two-month period, this
676 study documented the significant changes in auditory pathophysiology and a potential
677 multi-stage recovery process in animals exposed to a single mild blast trauma. We found
678 that hearing thresholds largely recovered except for broadband stimuli, and some aspects
679 of lasting deficits could be explained by threshold shifts. Recovery of temporal processing
680 of AM sounds was confined to lower modulation frequencies (<50 Hz), with responses
681 dependent on time point, sound level, noise masking, and AMF. More complex, speech-
682 like stimuli (IRN) demonstrated lasting deficits, pointing towards more effective stimuli for
683 elucidating the behavioral difficulties in human and animal listeners.
684

685 ## Acknowledgments

686 The authors would like to thank Jonathan Tang, Brandon Coventry, Alex Sommers,
687 Nanami Miyazaki, and all the other members in Central Auditory Processing Lab and Lab
688 of Translational Neuroscience for their generous assistance in the completion of this study.
689

690 ## Author contributions

691 Study concept and design: Edward Bartlett, Riyi Shi, Emily X. Han, Joseph M. Fernandez.

692 Animal Blast Exposure: Joseph M. Fernandez.

693 Electrophysiology: Emily X. Han, Caitlin Swanberg.

694 Data analysis and interpretation: Emily X. Han, Edward Bartlett, Joseph M. Fernandez.

695 Writing of the manuscript: Emily X. Han, Edward Bartlett.

696 Critical revision of the manuscript: Riyi Shi, Joseph M. Fernandez, Caitlin Swanberg.

697 Study supervision and obtainment of funding: Edward Bartlett, Riyi Shi.

698

699 **Funding**

700 This study is funded by Indiana CTSI 11917.

701

702 **Disclosures**

703 Riyi Shi is a co-founder of Neuro Vigor, a company developing novel drug treatments

704 and diagnostic approaches for neurodegenerative diseases and neurotrauma.

705

References

Alsindi S, **Patterson RD**, **Sayles M**, **Winter IM**. The responses of single units to simple and complex sounds from the superior olivary complex of the Guinea pig. In: *Acta Acustica united with Acustica*. S. Hirzel Verlag GmbH, 2018, p. 856–859.

Alvarado JC, **Fuentes-Santamaría V**, **Jareño-Flores T**, **Blanco JL**, **Juiz JM**. Normal variations in the morphology of auditory brainstem response (ABR) waveforms: A study in wistar rats. *Neurosci Res* 73: 302–311, 2012.

Anderson S, **Parbery-Clark A**, **White-Schwoch T**, **Kraus N**. Auditory brainstem response to complex sounds predicts self-reported speech-in-noise performance. *J Speech, Lang Hear Res* 56: 31–43, 2013.

Anderson S, **Skoe E**, **Chandrasekaran B**, **Kraus N**. Neural timing is linked to speech perception in noise. *J Neurosci* 30: 4922–4926, 2010.

Barth DS, **Shi Di**. The functional anatomy of middle latency auditory evoked potentials. *Brain Res* 565: 109–115, 1991.

Bendor D, **Wang X**. The neuronal representation of pitch in primate auditory cortex. *Nature* 436: 1161–1165, 2005.

Berger G, **Finkelstein Y**, **Avraham S**, **Himmelfarb M**. Patterns of hearing loss in non-explosive blast injury of the ear. *J Laryngol Otol* 111: 1137–1141, 1997.

Bharadwaj HM, **Masud S**, **Mehraei G**, **Verhulst S**, **Shinn-Cunningham BG**. Individual differences reveal correlates of hidden hearing deficits. *J Neurosci* 35: 2161–2172, 2015.

Bidelman GM, **Villafuerte JW**, **Moreno S**, **Alain C**. Age-related changes in the subcortical-cortical encoding and categorical perception of speech. *Neurobiol Aging*

728 35: 2526–2540, 2014.

729 **Bramhall NF**, **Niemczak CE**, **Kampel SD**, **Billings CJ**, **McMillan GP**. Evoked Potentials
730 Reveal Noise Exposure–Related Central Auditory Changes Despite Normal Audiograms.
731 *Am J Audiol* 29: 152–164, 2020.

732 **Bressler S**, **Goldberg H**, **Shinn-Cunningham B**. Sensory coding and cognitive processing
733 of sound in Veterans with blast exposure. *Hear Res* 349: 98–110, 2017.

734 **Brett B**, **Krishnan G**, **Barth DS**. The effects of subcortical lesions on evoked potentials and
735 spontaneous high frequency (gamma-band) oscillating potentials in rat auditory cortex.
736 *Brain Res* 721: 155–166, 1996.

737 **Caspary DM**, **Ling L**, **Turner JG**, **Hughes LF**. Inhibitory neurotransmission, plasticity and
738 aging in the mammalian central auditory system. *J Exp Biol* 211: 1781–1791, 2008.

739 **Caspary DM**, **Schatteman T a**, **Hughes LF**. Age-related changes in the inhibitory
740 response properties of dorsal cochlear nucleus output neurons: role of inhibitory inputs.
741 *J Neurosci* 25: 10952–9, 2005.

742 **Cave K**, **Cornish EM**, **Chandler DW**. Blast Injury of the Ear: Clinical Update from the
743 Global War on Terror. *Mil Med* 172: 726–730, 2007.

744 **Chavko M**, **Watanabe T**, **Adeeb S**, **Lankasky J**, **Ahlers ST**, **McCarron RM**. Relationship
745 between orientation to a blast and pressure wave propagation inside the rat brain. *J*
746 *Neurosci Methods* 195: 61–66, 2011.

747 **Cho HJ**, **Sajja VSSS**, **VandeVord PJ**, **Lee YW**. Blast induces oxidative stress, inflammation,
748 neuronal loss and subsequent short-term memory impairment in rats. *Neuroscience*
749 253: 9–20, 2013a.

750 Cho S Il, Gao SS, Xia A, Wang R, Salles FT, Raphael PD, Abaya H, Wachtel J, Baek J,
751 Jacobs D, Rasband MN, Oghalai JS. Mechanisms of Hearing Loss after Blast Injury to the
752 Ear. *PLoS One* 8, 2013b.
753 Cohen JT, Ziv G, Bloom J, Zikk D, Rapoport Y, Himmelfarb MZ. Blast injury of the ear in a
754 confined space explosion: Auditory and vestibular evaluation. *Isr Med Assoc J* 4: 559–
755 562, 2002.
756 Dal Cengio Leonardi A, Keane NJ, Bir CA, Ryan AG, Xu L, VandeVord PJ. Head
757 orientation affects the intracranial pressure response resulting from shock wave loading
758 in the rat. *J Biomech* 45: 2595–2602, 2012.
759 Deiber MP, Ibañez V, Fischer C, Perrin F, Mauguière F. Sequential mapping favours the
760 hypothesis of distinct generators for Na and Pa middle latency auditory evoked
761 potentials. *Electroencephalogr Clin Neurophysiol Evoked Potentials* 71: 187–197, 1988.
762 DePalma RG, Burris DG, Champion HR, Hodgson MJ. Current concepts: Blast injuries. *N.*
763 *Engl. J. Med.* 352Massachusetts Medical Society: 1335–1342, 2005.
764 Di S, Barth DS. The functional anatomy of middle-latency auditory evoked potentials:
765 Thalamocortical connections. *J Neurophysiol* 68: 425–431, 1992.
766 Du X, Ewert DL, Cheng W, West MB, Lu J, Li W, Floyd RA, Kopke RD. Effects of
767 antioxidant treatment on blast-induced brain injury. *PLoS One* 8: e80138, 2013.
768 Ewert DL, Lu J, Li W, Du X, Floyd R, Kopke R. Antioxidant treatment reduces blast-
769 induced cochlear damage and hearing loss. *Hear Res* 285: 29–39, 2012.
770 Fulbright ANC, Le Prell CG, Griffiths SK, Lobarinas E. Effects of Recreational Noise on
771 Threshold and Suprathreshold Measures of Auditory Function. *Semin Hear* 38: 298–318,

2017.

Gallun FJ, Diedesch AC, Kubli LR, Walden TC, Folmer RL, Samantha Lewis S, McDermott DJ, Fausti SA, Leek MR. Performance on tests of central auditory processing by individuals exposed to high-intensity blasts. *J Rehabil Res Dev* 49: 1005–1024, 2012a.

Gallun FJ, Lewis MS, Folmer RL, Diedesch AC, Aud ;, Kubli LR, McDermott DJ, Walden TC, Fausti S a, Lew HL, Leek MR. Implications of blast exposure for central auditory function: a review. *J Rehabil Res Dev* 49: 1059–74, 2012b.

Garman RH, Jenkins LW, Switzer RC, Bauman RA, Tong LC, Swauger P V., Parks SA, Ritzel D V., Dixon CE, Clark RSB, Bayır H, Kagan V, Jackson EK, Kochanek PM. Blast Exposure in Rats with Body Shielding Is Characterized Primarily by Diffuse Axonal Injury. *J Neurotrauma* 28: 947–959, 2011.

Greenhouse SW, Geisser S. On methods in the analysis of profile data. *Psychometrika* 24: 95–112, 1959.

Grinn SK, Wiseman KB, Baker JA, Le Prell CG. Hidden hearing loss? No effect of common recreational noise exposure on cochlear nerve response amplitude in humans. *Front Neurosci* 11: 465, 2017.

Guest H, Munro KJ, Prendergast G, Millman RE, Plack CJ. Impaired speech perception in noise with a normal audiogram: No evidence for cochlear synaptopathy and no relation to lifetime noise exposure. *Hear Res* 364: 142–151, 2018.

Van Haesendonck G, Van Rompaey V, Gilles A, Topsakal V, Van de Heyning P. Otologic Outcomes After Blast Injury: The Brussels Bombing Experience. *Otol Neurotol* 39: 1250–1255, 2018.

794 **Hamann K**, **Durkes A**, **Ouyang H**, **Uchida K**, **Pond A**, **Shi R**. Critical role of acrolein in
795 secondary injury following ex vivo spinal cord trauma. *J Neurochem* 107: 712–721, 2008.
796 **Herrmann B**, **Buckland C**, **Johnsrude IS**. Neural signatures of temporal regularity
797 processing in sounds differ between younger and older adults. *Neurobiol Aging* 83: 73–
798 85, 2019.
799 **Hickox AE**, **Liberman MC**. Is noise-induced cochlear neuropathy key to the generation
800 of hyperacusis or tinnitus? *J Neurophysiol* 111: 552–564, 2014.
801 **Holmes E**, **Griffiths TD**. 'Normal' hearing thresholds and fundamental auditory grouping
802 processes predict difficulties with speech-in-noise perception. *Sci Rep* 9: 1–11, 2019.
803 **Hua Y**, **Wang Y**, **Gu L**. Primary blast waves induced brain dynamics influenced by head
804 orientations. *Biomed Eng Lett* 7: 253–259, 2017.
805 **Joris PX**, **Schreiner CE**, **Rees A**. *Neural Processing of Amplitude-Modulated Sounds*.
806 American Physiological Society, 2004.
807 **Kerr AG**. The effects of blast on the ear. *J Laryngol Otol* 94: 107–110, 1980.
808 **Knudsen SK**, **Øen EO**. Blast-induced neurotrauma in whales. *Neurosci Res* 46: 377–386,
809 2003.
810 **Krishnan A**, **Gandour JT**, **Suresh CH**. Cortical pitch response components show
811 differential sensitivity to native and nonnative pitch contours. *Brain Lang* 138: 51–60,
812 2014.
813 **Krishnan A**, **Gandour JT**, **Suresh CH**. Pitch processing of dynamic lexical tones in the
814 auditory cortex is influenced by sensory and extrasensory processes. *Eur J Neurosci* 41:
815 1496–1504, 2015.

816 Krishnan A, Gandour JT, Xu Y, Suresh CH. Language-dependent changes in pitch-
817 relevant neural activity in the auditory cortex reflect differential weighting of temporal
818 attributes of pitch contours. *J Neurolinguistics* 41: 38–49, 2017a.
819 Krishnan A, Suresh CH, Gandour JT. Changes in pitch height elicit both language-
820 universal and language-dependent changes in neural representation of pitch in the
821 brainstem and auditory cortex. *Neuroscience* 346: 52–63, 2017b.
822 Kubli LR, Brungart D, Northern J. Effect of Blast Injury on Auditory Localization in Military
823 Service Members. *Ear Hear* 39: 457–469, 2018.
824 Kujawa SG, Liberman MC. Synaptopathy in the noise-exposed and aging cochlea:
825 Primary neural degeneration in acquired sensorineural hearing loss. *Hear Res* 330: 191–
826 199, 2015.
827 Lai J, Bartlett EL. Age-related shifts in distortion product otoacoustic emissions peak-
828 ratios and amplitude modulation spectra. *Hear Res* 327: 186–198, 2015.
829 Lai J, Bartlett EL. Masking Differentially Affects Envelope-following Responses in Young
830 and Aged Animals. *Neuroscience* 386: 150–165, 2018.
831 Lai J, Sommer AL, Bartlett EL. Age-related changes in envelope-following responses at
832 equalized peripheral or central activation. *Neurobiol Aging* 58: 191–200, 2017.
833 Laplaca MC, Lee VMY, Thibault LE. An in vitro model of traumatic neuronal injury:
834 Loading rate-dependent changes in acute cytosolic calcium and lactate dehydrogenase
835 release. *J Neurotrauma* 14: 355–368, 1997.
836 Leung LY, VandeVord PJ, Dal Cengio AL, Bir C, Yang KH, King AI. Blast related
837 neurotrauma: A review of cellular injury. *MCB Mol. Cell. Biomech.* 5: 155–168, 2008.

838 Lew HL, Garvert DW, Pogoda TK, Hsu P Te, Devine JM, White DK, Myers PJ, Goodrich
839 GL. Auditory and visual impairments in patients with blast-related traumatic brain injury:
840 Effect of dual sensory impairment on functional independence measure. *J Rehabil Res*
841 *Dev* 46: 819–826, 2009.
842 Liberman MC. Noise-induced and age-related hearing loss: New perspectives and
843 potential therapies. *F1000Research* 6: 1–11, 2017.
844 Liégeois-Chauvel C, Musolino A, Badier JM, Marquis P, Chauvel P. Evoked potentials
845 recorded from the auditory cortex in man: evaluation and topography of the middle
846 latency components. *Electroencephalogr Clin Neurophysiol Evoked Potentials* 92: 204–
847 214, 1994.
848 Luo H, Pace E, Zhang X, Zhang J. Blast-Induced tinnitus and spontaneous firing changes
849 in the rat dorsal cochlear nucleus. *J Neurosci Res* 92: 1466–1477, 2014a.
850 Luo H, Pace E, Zhang X, Zhang J. Blast-induced tinnitus and spontaneous activity
851 changes in the rat inferior colliculus. *Neurosci Lett* 580: 47–51, 2014b.
852 Mahmood G, Mei Z, Hojjat H, Pace E, Kallakuri S, Zhang JS. Therapeutic effect of
853 sildenafil on blast-induced tinnitus and auditory impairment. *Neuroscience* 269: 367–
854 382, 2014.
855 Manzoor NF, Gao Y, Licari F, Kaltenbach JA. Comparison and contrast of noise-induced
856 hyperactivity in the dorsal cochlear nucleus and inferior colliculus. *Hear Res* 295: 114–
857 123, 2013.
858 Mao JC, Pace E, Pierozynski P, Kou Z, Shen Y, Vandevord P, Haacke EM, Zhang X, Zhang
859 J. Blast-induced tinnitus and hearing loss in rats: Behavioral and imaging assays. *J*

860 *Neurotrauma* 29: 430–444, 2012a.

861 Mao JC, Pace E, Pierozynski P, Kou Z, Shen Y, VandeVord P, Haacke EM, Zhang X,

862 Zhang J. Blast-Induced Tinnitus and Hearing Loss in Rats: Behavioral and Imaging

863 Assays. *J Neurotrauma* 29: 430–444, 2012b.

864 Masri S, Zhang LS, Luo H, Pace E, Zhang J, Bao S. Blast Exposure Disrupts the Tonotopic

865 Frequency Map in the Primary Auditory Cortex. *Neuroscience* 379: 428–434, 2018.

866 McGee T, Kraus N. Auditory development reflected by middle latency response. *Ear*

867 *Hear* 17: 419–429, 1996.

868 McGee T, Kraus N, Comperatore C, Nicol T. Subcortical and cortical components of the

869 MLR generating system. *Brain Res* 544: 211–220, 1991.

870 McGee T, Kraus N, Littman T, Nicol T. Contributions of medial geniculate body

871 subdivisions to the middle latency response. *Hear Res* 61: 147–154, 1992.

872 Meehan A, Hebert D, Deru K, Weaver LK. Longitudinal study of hyperbaric oxygen

873 intervention on balance and affective symptoms in military service members with

874 persistent post-concussive symptoms. *J Vestib Res Equilib Orientat* 29: 205–219, 2019.

875 Mulders WHAM, Ding D, Salvi R, Robertson D. Relationship between auditory

876 thresholds, central spontaneous activity, and hair cell loss after acoustic trauma. *J Comp*

877 *Neurol* 519: 2637–2647, 2011.

878 Mulders WHAM, Robertson D. Hyperactivity in the auditory midbrain after acoustic

879 trauma: dependence on cochlear activity. *Neuroscience* 164: 733–746, 2009.

880 Mulders WHAM, Robertson D. Progressive centralization of midbrain hyperactivity after

881 acoustic trauma. *Neuroscience* 192: 753–760, 2011.

882 **Mulders WHAM**, **Robertson D**. Development of hyperactivity after acoustic trauma in
883 the guinea pig inferior colliculus. *Hear Res* 298: 104–108, 2013.
884 **Musiek F**, **Nagle S**. The middle latency response: A review of findings in various central
885 nervous system lesions. *J. Am. Acad. Audiol.* 29American Academy of Audiology: 855–
886 867, 2018.
887 **Parthasarathy A**, **Bartlett E**. Two-channel recording of auditory-evoked potentials to
888 detect age-related deficits in temporal processing. *Hear Res* 289: 52–62, 2012.
889 **Parthasarathy A**, **Bartlett EL**. Age-related auditory deficits in temporal processing in F-
890 344 rats. *Neuroscience* 192: 619–630, 2011.
891 **Parthasarathy A**, **Cunningham PA**, **Bartlett EL**. Age-related differences in auditory
892 processing as assessed by amplitude-modulation following responses in quiet and in
893 noise. *Front Aging Neurosci* 2: 152, 2010.
894 **Parthasarathy A**, **Datta J**, **Torres JAL**, **Hopkins C**, **Bartlett EL**. Age-related changes in the
895 relationship between auditory brainstem responses and envelope-following responses.
896 *JARO - J Assoc Res Otolaryngol* 15: 649–661, 2014.
897 **Parthasarathy A**, **Lai J**, **Bartlett EL**. Age-Related Changes in Processing Simultaneous
898 Amplitude Modulated Sounds Assessed Using Envelope Following Responses. *JARO - J*
899 *Assoc Res Otolaryngol* 17: 119–132, 2016.
900 **Patterson JH**, **Hamernik RP**. Blast overpressure induced structural and functional
901 changes in the auditory system. 1997.
902 **Patterson RD**, **Handel S**, **Yost WA**, **Jaysurya Datta A**. The relative strength of the tone
903 and noise components in iterated rippled noise. *J Acoust Soc Am* 100: 3286–3294, 1996.

904 **Peter V**, **Wong K**, **Narne VK**, **Sharma M**, **Purdy SC**, **McMahon C**. Assessing spectral and
905 temporal processing in children and adults using Temporal Modulation Transfer
906 Function (TMTF), Iterated Ripple Noise (IRN) perception, and Spectral Ripple
907 Discrimination (SRD). *J Am Acad Audiol* 25: 210–218, 2014.
908 **Phillips DJ**, **Schei JL**, **Meighan PC**, **Rector DM**. State-Dependent Changes in Cortical Gain
909 Control as Measured by Auditory Evoked Responses to Varying Intensity Stimuli. *Sleep*
910 34: 1527–1537, 2011.
911 **Plack CJ**, **Barker D**, **Prendergast G**. Perceptual consequences of "hidden" hearing loss.
912 *Trends Hear* 18: 233121651455062, 2014.
913 **Rabang CF**, **Parthasarathy A**, **Venkataraman Y**, **Fisher ZL**, **Gardner SM**, **Bartlett EL**. A
914 computational model of inferior colliculus responses to amplitude modulated sounds in
915 young and aged rats. *Front Neural Circuits* 6: 77, 2012.
916 **Race N**, **Lai J**, **Shi R**, **Bartlett EL**. Differences in postinjury auditory system
917 pathophysiology after mild blast and nonblast acute acoustic trauma. *J Neurophysiol*
918 118: 782–799, 2017.
919 **Rafaels K**, **"Dale" Bass CR**, **Salzar RS**, **Panzer MB**, **Woods W**, **Feldman S**, **Cummings T**,
920 **Capehart B**. Survival Risk Assessment for Primary Blast Exposures to the Head. *J*
921 *Neurotrauma* 28: 2319–2328, 2011.
922 **Remenschneider AK**, **Lookabaugh S**, **Aliphas A**, **Brodsky JR**, **Devaiah AK**, **Dagher W**,
923 **Grundfast KM**, **Heman-Ackah SE**, **Rubin S**, **Sillman J**, **Tsai AC**, **Vecchiotti M**, **Kujawa SG**,
924 **Lee DJ**, **Quesnel AM**. Otologic outcomes after blast injury: The Boston Marathon
925 experience. *Otol Neurotol* 35: 1825–1834, 2014.

926 Ritenour AE, Wickley A, Ritenour JS, Kriete BR, Blackbourne LH, Holcomb JB, Wade CE.
927 Tympanic membrane perforation and hearing loss from blast overpressure in Operation
928 Enduring Freedom and Operation Iraqi Freedom wounded. *J Trauma* 64, 2008.
929 Robertson D, Bester C, Vogler D, Mulders WHAM. Spontaneous hyperactivity in the
930 auditory midbrain: Relationship to afferent input. *Hear Res* 295: 124–129, 2013.
931 Rosen S. Temporal information in speech: acoustic, auditory and linguistic aspects.
932 *Philos. Trans. R. Soc. Lond. B. Biol. Sci.* 336The Royal Society London: 367–373, 1992.
933 Säljö A, Mayorga M, Bolouri H, Svensson B, Hamberger A. Mechanisms and
934 pathophysiology of the low-level blast brain injury in animal models. *Neuroimage* 54:
935 S83–S88, 2011.
936 Saunders GH, Frederick MT, Arnold M, Silverman S, Chisolm TH, Myers P. Auditory
937 difficulties in blast-exposed veterans with clinically normal hearing. *J Rehabil Res Dev*
938 52: 343–360, 2015.
939 Shearer DE, Molis MR, Bennett KO, Leek MR. impaired listeners by normal-hearing and
940 hearing-impaired listeners a). 378, 2018.
941 Simpson G V., Knight RT, Brailowsky S, Prospero-Garcia O, Scabini D. Altered peripheral
942 and brainstem auditory function in aged rats. *Brain Res* 348: 28–35, 1985.
943 Simpson MIG, Prendergast G. Auditory magnetic evoked responses. In: *Handbook of*
944 *Clinical Neurophysiology*. 2013, p. 253–270.
945 Skoe E, Kraus N. Auditory Brain Stem Response to Complex Sounds: A Tutorial. *Ear Hear*
946 31: 302–324, 2010.
947 Song S, Race NS, Kim A, Zhang T, Shi R, Ziaie B. A Wireless Intracranial Brain

948 Deformation Sensing System for Blast-Induced Traumatic Brain Injury. *Sci Rep* 5: 1–10,
949 2015.
950 **Sun W**, **Deng A**, **Jayaram A**, **Gibson B**. Noise exposure enhances auditory cortex
951 responses related to hyperacusis behavior. *Brain Res* 1485: 108–116, 2012.
952 **Šuta D**, **Rybalko N**, **Pelánová J**, **Popelář J**, **Syka J**. Age-related changes in auditory
953 temporal processing in the rat. *Exp Gerontol* 46: 739–746, 2011.
954 **Swaminathan J**, **Krishnan A**, **Gandour JT**. Pitch encoding in speech and nonspeech
955 contexts in the human auditory brainstem. *Neuroreport* 19: 1163–1167, 2008.
956 **Syka J**, **Rybalko N**. Threshold shifts and enhancement of cortical evoked responses after
957 noise exposure in rats. *Hear Res* 139: 59–68, 2000.
958 **Tichko P**, **Skoe E**. Frequency-dependent fine structure in the frequency-following
959 response: The byproduct of multiple generators. *Hear Res* 348: 1–15, 2017.
960 **Tukey JW**. Comparing Individual Means in the Analysis of Variance. *Biometrics* 5: 99,
961 1949.
962 **Unnikrishnan G**, **Mao H**, **Sundaramurthy A**, **Bell ED**, **Yeoh S**, **Monson K**, **Reifman J**. A 3-D
963 Rat Brain Model for Blast-Wave Exposure: Effects of Brain Vasculature and Material
964 Properties. *Ann Biomed Eng* 47: 2033–2044, 2019.
965 **Valderrama JT**, **Beach EF**, **Yeend I**, **Sharma M**, **Van Dun B**, **Dillon H**. Effects of lifetime
966 noise exposure on the middle-age human auditory brainstem response, tinnitus and
967 speech-in-noise intelligibility. *Hear Res* 365: 36–48, 2018.
968 **Viana LM**, **O'Malley JT**, **Burgess BJ**, **Jones DD**, **Oliveira CACP**, **Santos F**, **Merchant SN**,
969 **Liberman LD**, **Liberman MC**. Cochlear neuropathy in human presbycusis: Confocal

970 analysis of hidden hearing loss in post-mortem tissue. *Hear Res* 327: 78–88, 2015.

971 **Wagner L**, **Plontke SK**, **Rahne T**. Perception of Iterated Rippled Noise Periodicity in

972 Cochlear Implant Users. *Audiol Neurotol* 22: 104–115, 2017.

973 **Walls MK**, **Race N**, **Zheng L**, **Vega-Alvarez SM**, **Acosta G**, **Park J**, **Shi R**. Structural and

974 biochemical abnormalities in the absence of acute deficits in mild primary blast-induced

975 head trauma. *J Neurosurg* 124: 675–686, 2016.

976 **Walton JP**. Timing is everything: Temporal processing deficits in the aged auditory

977 brainstem. *Hear Res* 264: 63–69, 2010.

978 **Wang H**, **Turner JG**, **Ling L**, **Parrish JL**, **Hughes LF**, **Caspary DM**. Age-related changes in

979 glycine receptor subunit composition and binding in dorsal cochlear nucleus.

980 *Neuroscience* 160: 227–239, 2009.

981 **Wang X**, **Lu T**, **Bendor D**, **Bartlett E**. Neural coding of temporal information in auditory

982 thalamus and cortex. *Neuroscience* 154: 294–303, 2008.

983 **Vander Werff KR**. Auditory Dysfunction Among Long-Term Consequences of Mild

984 Traumatic Brain Injury (mTBI). *Perspect Hear Hear Disord Res Diagnostics* 16: 3, 2012.

985 **Yeend I**, **Beach EF**, **Sharma M**. Working Memory and Extended High-Frequency Hearing

986 in Adults: Diagnostic Predictors of Speech-in-Noise Perception. *Ear Hear* 40: 458–467,

987 2019.

988 **Yost WA**. Pitch of iterated rippled noise. *J Acoust Soc Am* 100: 511–518, 1996a.

989 **Yost WA**. Pitch strength of iterated rippled noise. *J Acoust Soc Am* 100: 3329–3335,

990 1996b.

991

Fig 1. Auditory evoked potential experiment setup and examples of ABR waveforms. A) Electrode placement and channel configuration of the study's auditory evoked potential experiment. B) Examples of ABR waveforms at 80 dB SPL and 30 dB SL, with relevant wave peaks labeled. The waves for which amplitudes are measured are labeled with a black triangle.

Fig 2. ABR threshold changes of Blast (N=10) and Sham (N=6) rats during the first two months post-exposure. Blast animals demonstrated drastic increases (worse) of Click, 8 kHz, and 16 kHz thresholds (red lines) post-exposure as opposed to Sham animals (blue lines). Significant main effects ($p \leqslant 0.001$) of Groups and Group*Time interactions were observed in all carriers. Significant Simple Main Effect of single time points observed in various carriers throughout the two months. For subsequent figures, red lines will denote blast-exposed animals, and blue lines will denote sham-exposed animals.

***Blast threshold significantly higher than Sham in Click, 8kHz, and 16kHz, $p<0.05$;

**Blast threshold significantly higher only in Click and 16 kHz;

*Blast threshold significantly higher only in Click.

Fig 3. ABR wave I, III, and V amplitudes of Blast (N=10) and Sham (N=6) rats during the first two months post-exposure expose persistent blast-induced differences at 80 dB SPL. Significant main Group*Time interaction effects ($p \leqslant 0.001$) observed in waves I (left column), III (center column), and V (right column) for all carriers: A) Click ABR; B) 8 kHz ABR; C) 16 kHz ABR. Click ABR revealed blast-induced reduction of ABR wave amplitudes

1015 to a greater degree than both tone ABRs. Later waves (Wave III and V) showed earlier
1016 recovery in Blast animals.
1017 *Significant Simple Main Effect of Group in ABR Wave Amplitudes, $p<0.05$.
1018
1019 **Fig 4. ABR wave I, III, and V amplitudes of Blast (N=10) and Sham (N=6) rats during the**
1020 **first two months post-exposure at 30 dB SL.** Similar format to Fig. 3. Significant main
1021 Group*Time interaction effects only observed with Click ABR waves (Wave I: $p=0.016$;
1022 Wave III: $p=0.04$; Wave V: $p=0.003$) A) Click ABR; B) 8 kHz ABR; C) 16 kHz ABR.
1023 *Significant Simple Main Effect of Group in ABR Wave Amplitudes, $p<0.05$.
1024
1025 **Fig 5. MLR waveforms and peak amplitudes of Blast (N=8) and Sham (N=6) rats during**
1026 **the first two months post-exposure at 80 dB SPL and at 30 dB SL (Thresh + 30 dB).** Grand
1027 average traces of Click MLR waveforms at 80 dB SPL: A) Blast, pre-blast to day 7.
1028 Arrowheads indicate measured peaks in E-H; B) Sham, pre-blast to day 7; C) Blast, day
1029 10 to day 60; D) Sham, day 10 to day 60. Normalized Click MLR wave amplitudes over
1030 time: E) Blast, 80 dB SPL; F) Sham, 80 dB SPL; G) Blast, 30 dB SL; H) Blast, 30 dB SL.
1031
1032 **Fig 6. AM depth stimuli and EFR responses from Blast (N=10) and Sham (N=6) rats during**
1033 **the first two months post-exposure at 30 dB above threshold, in quiet.** A) AM depth
1034 stimulus waveforms at 100% and 50% modulation depths; B) NAM FFT amplitudes at 10
1035 Hz (left), 45 Hz (center), and 256 Hz (right). Significant Group effect at 45Hz ($p=0.007$);
1036 Similar format in C and D. C) SAM 8 kHz FFT amplitudes at 45 Hz show a steady yet

1037 insignificant increase in later short-term (day 7-14); D) SAM 16k FFT amplitudes found

1038 no significant Group effect.

1039 **Significant Simple Main Effect of Group in FFT Amplitudes in both 100% depth and 50%

1040 depth

1041 * Significant Simple Main Effect of Group in FFT Amplitudes only in 100% depth

1042

1043 **Fig 7. AM noise stimuli and EFR responses from Blast (N=10) and Sham (N=6) rats during**

1044 **the first two months post-exposure at 30 dB above threshold.** A) AM noise stimulus

1045 composition and waveform. B) Amplitude modulated noise carrier. FFT amplitudes at

1046 signal modulation frequency in quiet and with 71 Hz AM noise masker level of 20SNR or

1047 0SNR (equal) show significant Noise * Group effect for: B) NAM noise at 45 Hz (p=0.011)

1048 modulation frequency; C) SAM 8 kHz noise at 10 Hz (p=0.001) and 45 Hz (p=0.015)

1049 modulation frequency.

1050 * Significant Simple Main Effect of Group

1051

1052 **Fig 8. IRN Chinese Tone stimuli and responses from Blast (N=8) and Sham (N=6) rats**

1053 **during the first two months post-exposure at 30 dB above threshold** A) Example

1054 waveform and spectrogram of IRN Tone 2 stimulus; B) Examples of Peak Frequency of

1055 IRN Evoked Potential in Pre-blast and Post-blast Brain (day 10 post-blast) from an

1056 individual animal; C) Significant effect of Group (*) was seen in IRN Tone 2 (top, p=0.026)

1057 and Tone 4 (bottom, p=0.029) pitch-tracking score, though Simple Main Effect of is

1058 limited for individual time points; D) Cross-correlation of post-blast IRN responses to

1059 corresponding pre-blast responses. Significant differences (*) in correlation coefficients
1060 to pre-blast responses between Blast and Sham were observed in two waves: day 1-10,
1061 and day 30 ($p<0.05$, paired sign-rank).
1062
1063 **Fig 9. Pitch tracking scores of responses to IRN Tone 2 stimuli with pitch salience**
1064 **controlled by altering iteration number at different time points, at 30 dB above threshold.**
1065 Though the effect of Iterations on pitch-tracking score was significant ($p<0.001$), no
1066 significant Iteration * Group interaction was observed.
1067
1068 **Table 1. Summary of 80 dB SPL ABR Wave I, III and V repeated measure ABR statistics.**
1069
1070 **Table 2. Summary of 30 dB SL ABR Wave I, III and V repeated measure ABR statistics.**
1071
1072 **Table 3. Simple main effects of blast group on ABR wave amplitudes over time.** Post-blast
1073 ABR amplitudes of Blast (N=10) and Sham (N=6) groups are compared using rmANOVA
1074 at each time point recorded. A $p<0.05$ showed significant simple main effect of Group at
1075 that time point.
1076
1077 **Table 4. Summary of post hoc tests against pre-blast ABR amplitudes.** Post-blast ABR
1078 amplitudes of Blast (N=10) and Sham (N=6) are compared against pre-blast amplitudes
1079 of the same group to show blast impact and recovery.

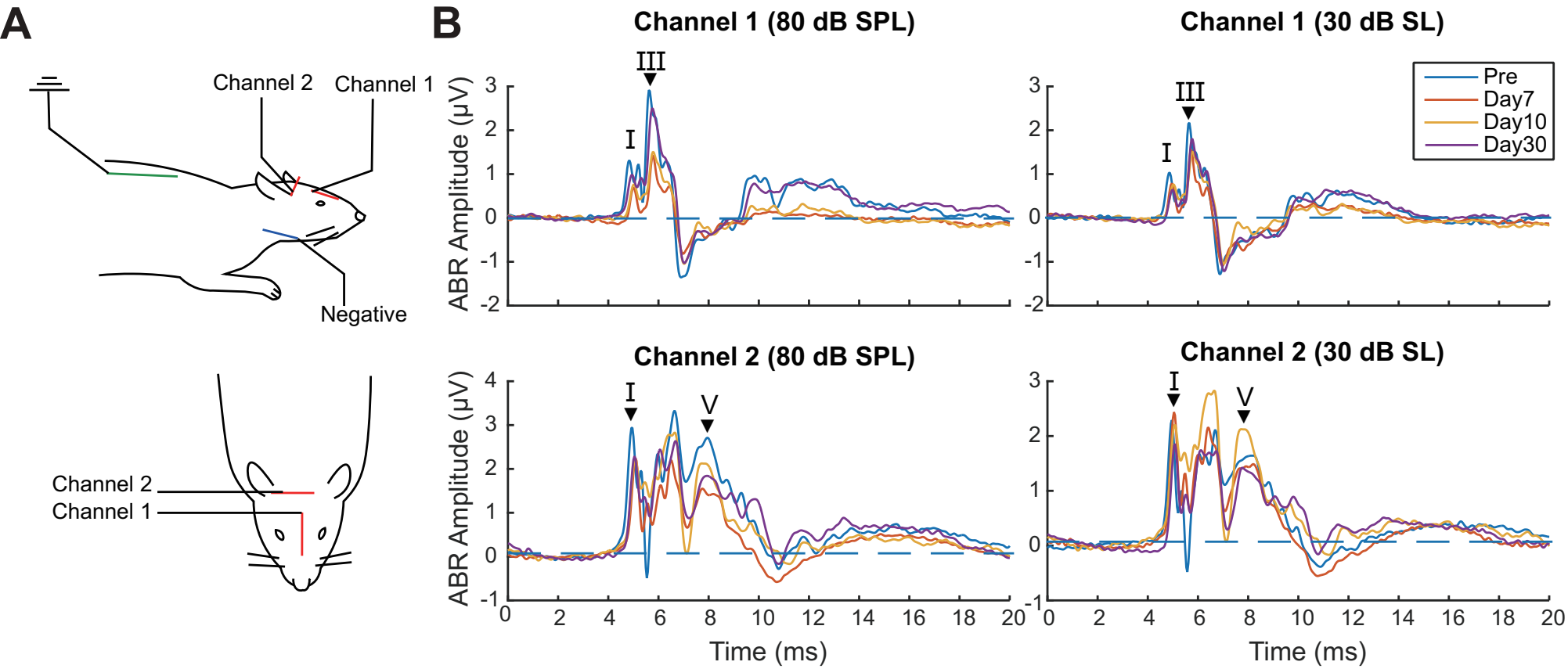
A
Channel 2
Channel 1
Negative
Channel 2
Channel 1
B
Channel 1 (80 dB SPL)
Channel 1 (30 dB SL)
Channel 2 (80 dB SPL)
Channel 2 (30 dB SL)
ABR Amplitude (μV)
Time (ms)
I
III
V
Pre
Day7
Day10
Day30

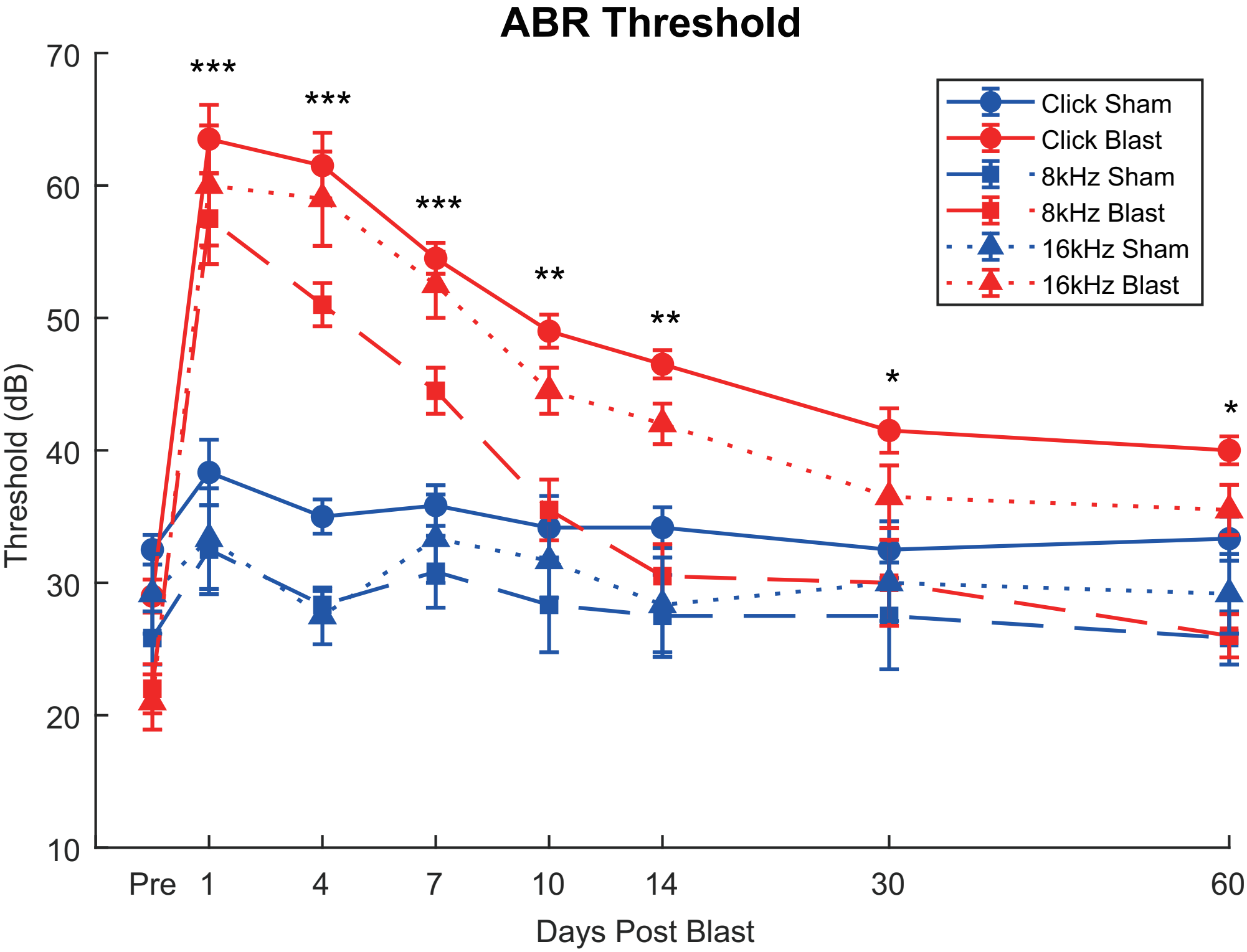
ABR Threshold
Threshold (dB)
70
60
50
40
30
20
10
***
***
***
**
**
*
*
Click Sham
Click Blast
8kHz Sham
8kHz Blast
16kHz Sham
16kHz Blast
Pre
1
4
7
10
14
30
60
Days Post Blast

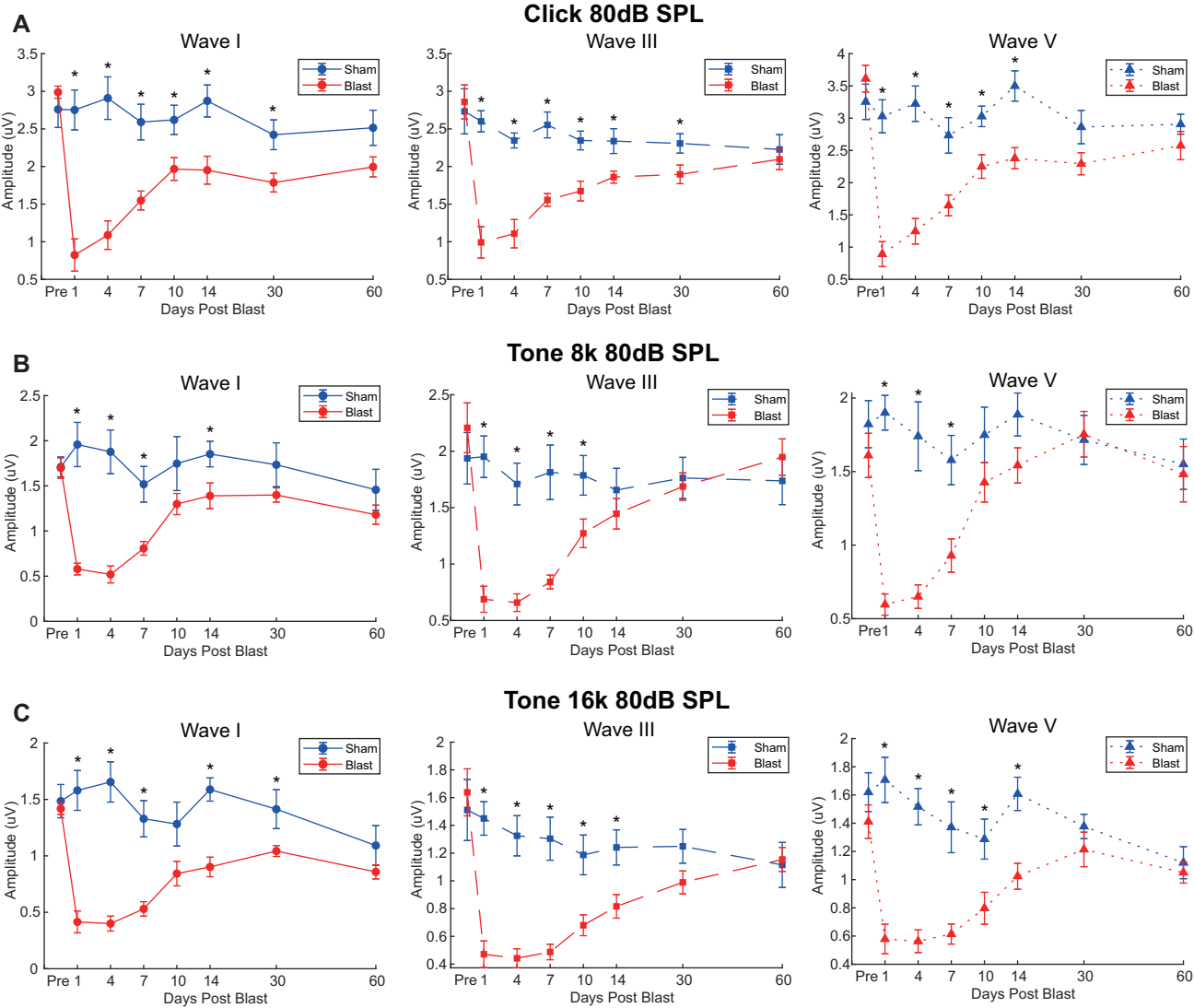
A
Click 80dB SPL
Wave I
Wave III
Wave V
Sham
Blast
Amplitude (uV)
Days Post Blast
Pre 1
4
7
10
14
30
60
B
Tone 8k 80dB SPL
C
Tone 16k 80dB SPL

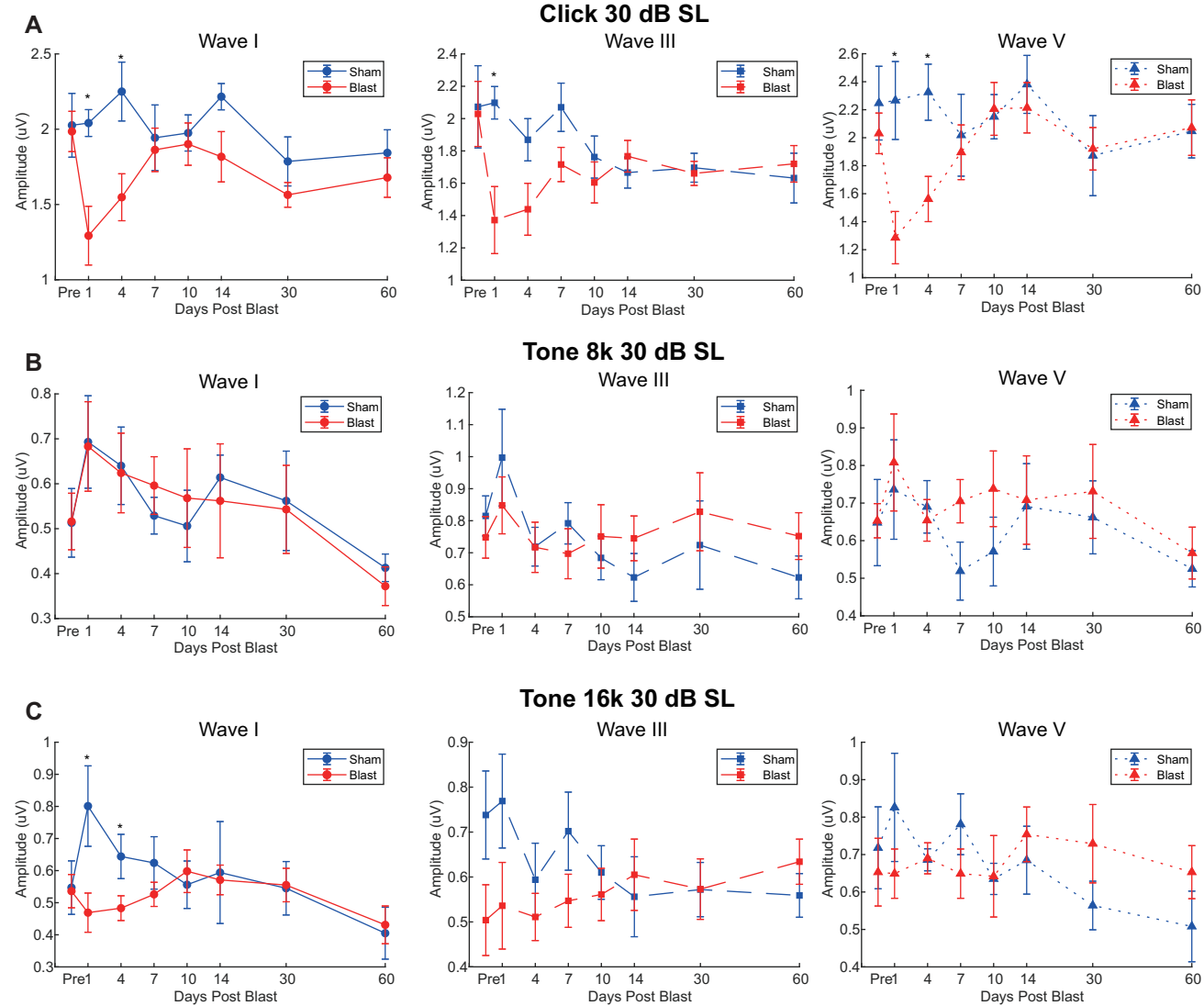
A
Click 30 dB SL
Wave I
Wave III
Wave V
Sham
Blast
Amplitude (uV)
Days Post Blast
Pre 1
4
7
10
14
30
60
B
Tone 8k 30 dB SL
C
Tone 16k 30 dB SL
Pre1

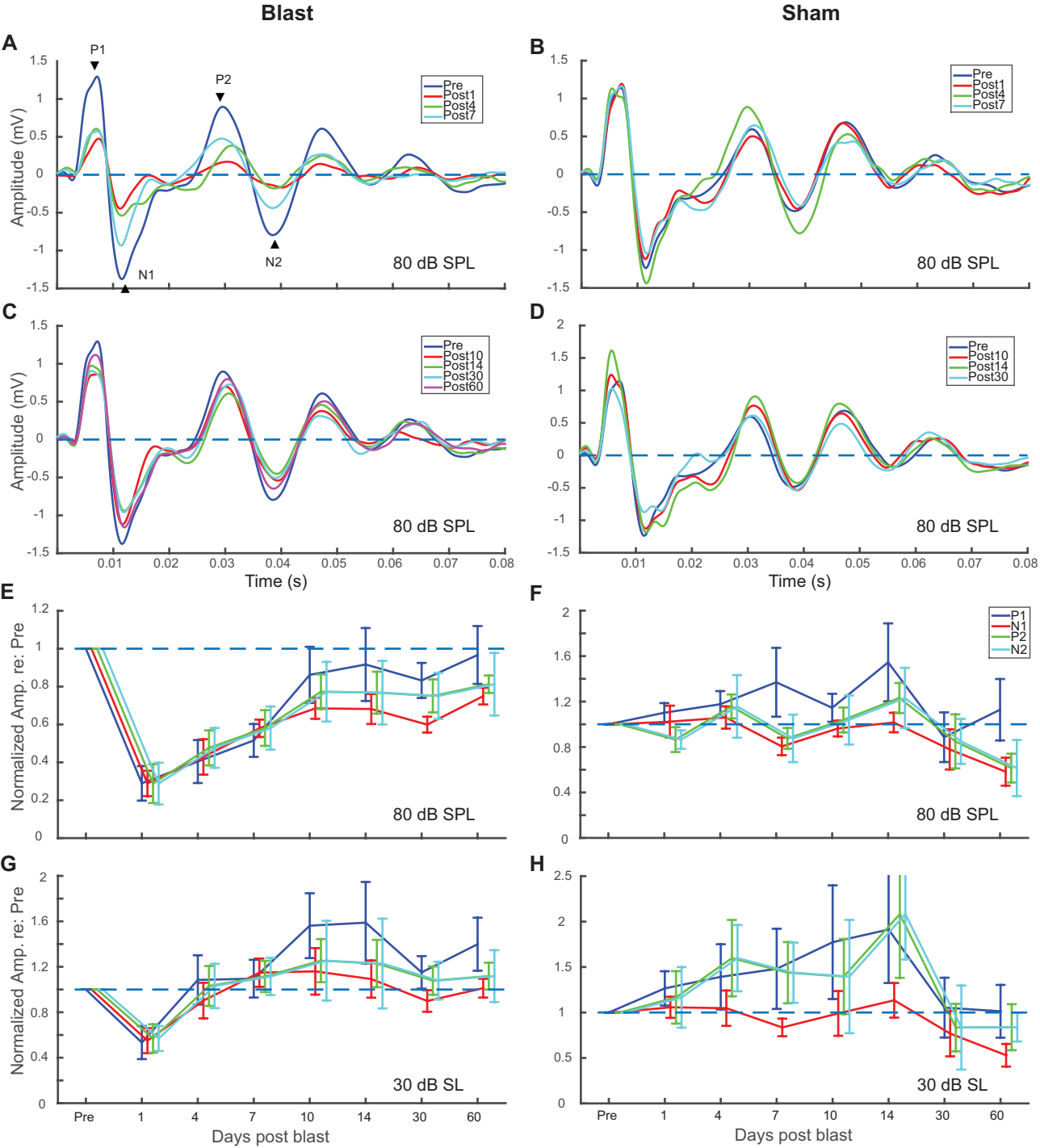
Blast
Sham
A
B
C
D
E
F
G
H
P1
P2
N1
N2
Pre
Post1
Post4
Post7
Post10
Post14
Post30
Post60
Amplitude (mV)
Time (s)
80 dB SPL
30 dB SL
Normalized Amp. re: Pre
Days post blast

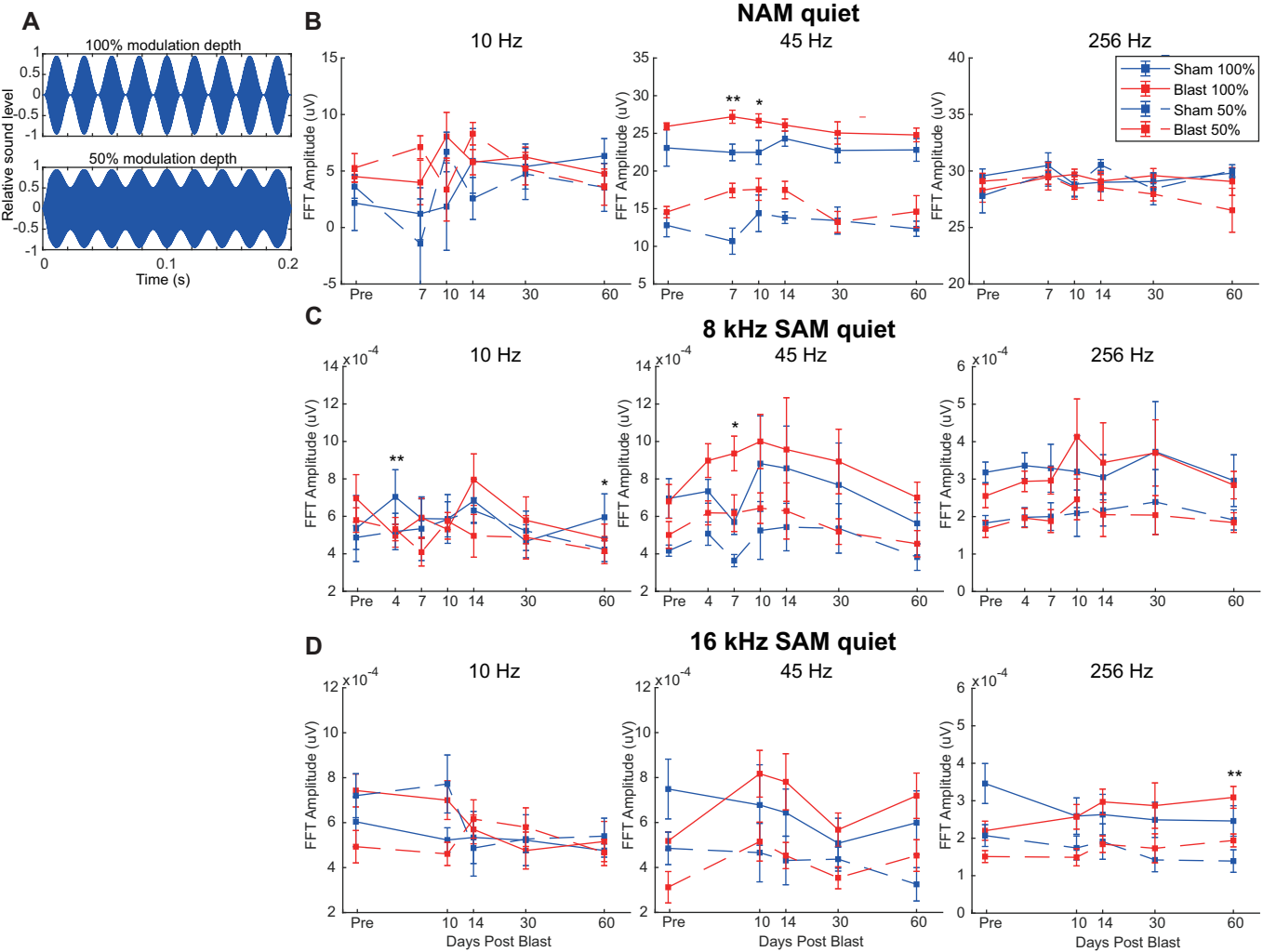
A
100% modulation depth
50% modulation depth
Relative sound level
Time (s)
B
NAM quiet
10 Hz
45 Hz
256 Hz
FFT Amplitude (uV)
Sham 100%
Blast 100%
Sham 50%
Blast 50%
C
8 kHz SAM quiet
D
16 kHz SAM quiet
Days Post Blast

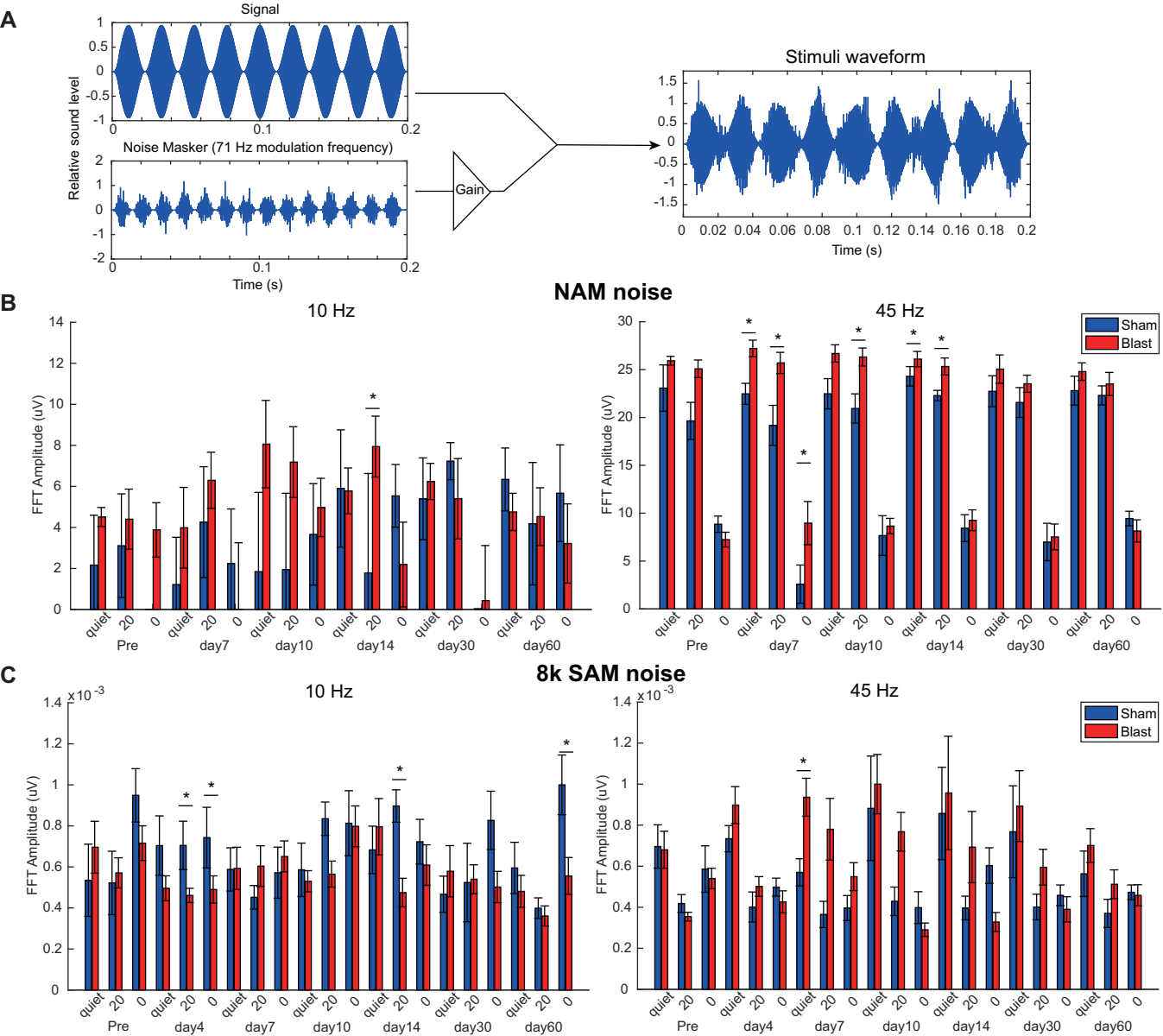
A
Signal
Relative sound level
Noise Masker (71 Hz modulation frequency)
Time (s)
Gain
Stimuli waveform
Time (s)
B
NAM noise
10 Hz
45 Hz
Sham
Blast
FFT Amplitude (uV)
quiet
20
0
Pre
day7
day10
day14
day30
day60
C
8k SAM noise
10 Hz
45 Hz
x10 -3
Sham
Blast
FFT Amplitude (uV)
Pre
day4
day7
day10
day14
day30
day60

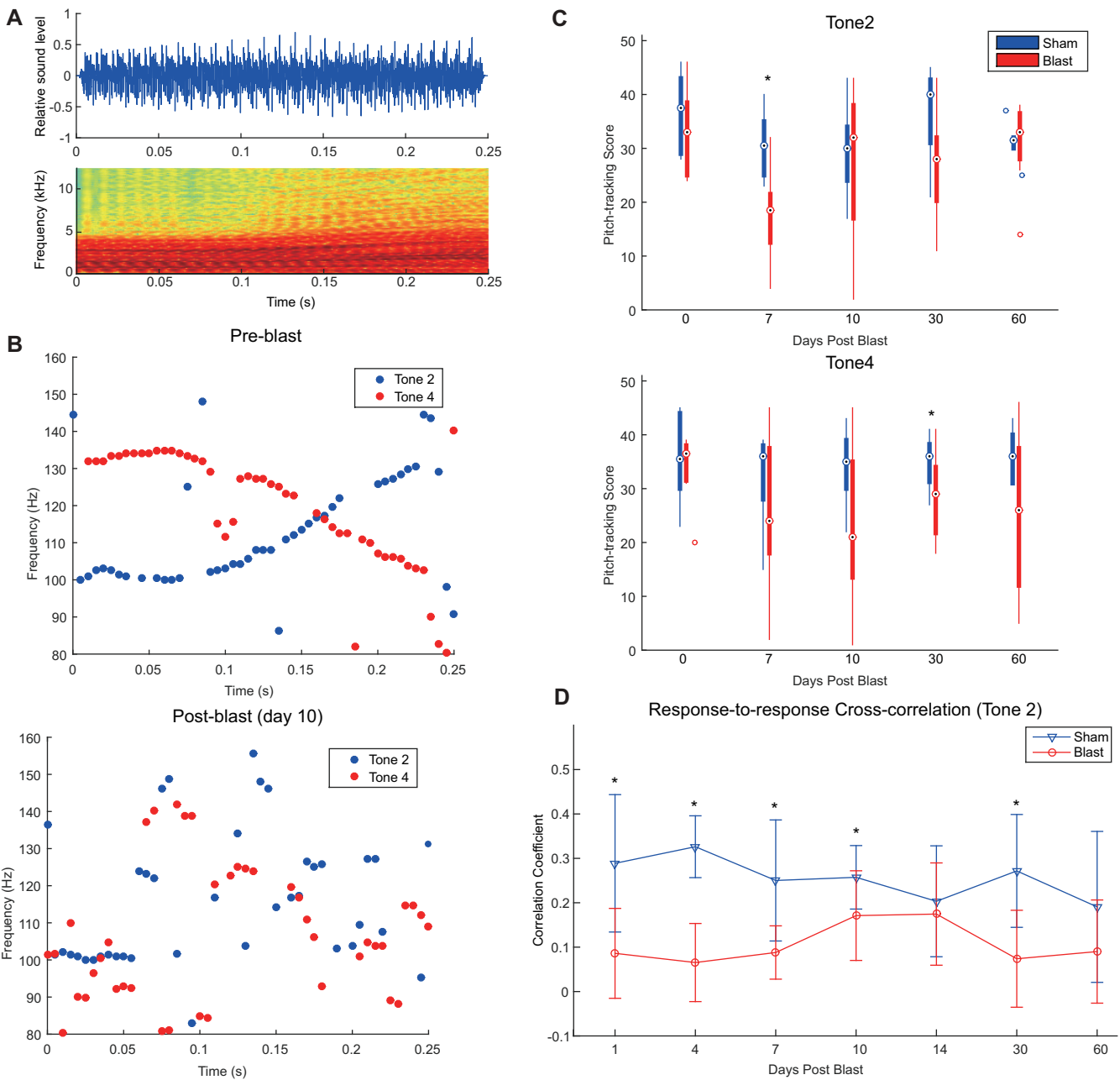
A
Relative sound level
Frequency (kHz)
Time (s)
B
Pre-blast
Tone 2
Tone 4
Frequency (Hz)
Time (s)
Post-blast (day 10)
Tone 2
Tone 4
Frequency (Hz)
Time (s)
C
Tone2
Sham
Blast
Pitch-tracking Score
Days Post Blast
Tone4
Pitch-tracking Score
Days Post Blast
D
Response-to-response Cross-correlation (Tone 2)
Sham
Blast
Correlation Coefficient
Days Post Blast

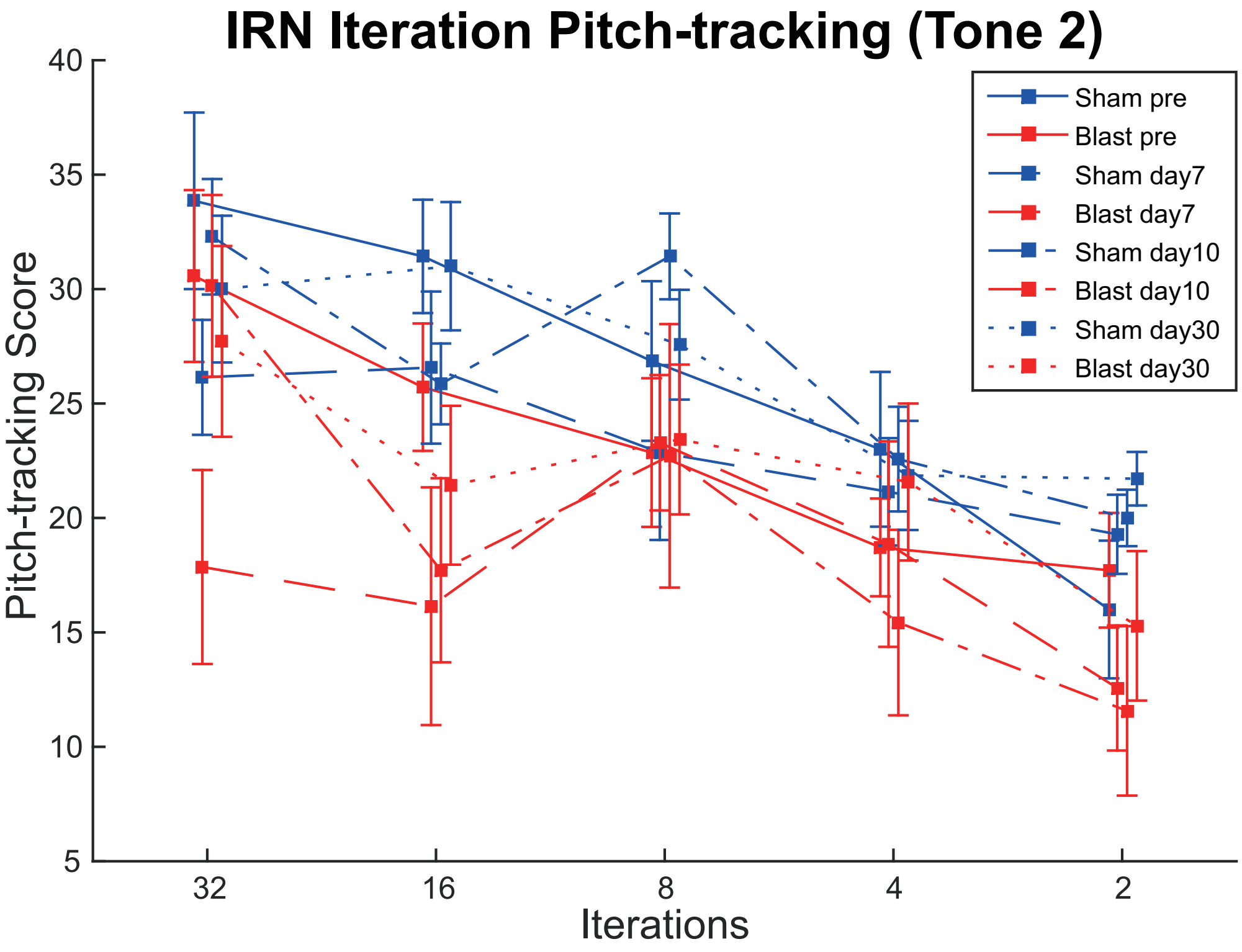
IRN Iteration Pitch-tracking (Tone 2)
Pitch-tracking Score
Iterations
40
35
30
25
20
15
10
5
32
16
8
4
2
Sham pre
Blast pre
Sham day7
Blast day7
Sham day10
Blast day10
Sham day30
Blast day30

Table 1

80dB ABR			F	p	η^2_p
Click	Wave I	Time	9.980	**< .001**	0.416
		Group	23.080	**< .001**	0.622
		Time * Group	11.685	**< .001**	0.455
	Wave III	Time	11.065	**< .001**	0.441
		Group	17.207	**< .001**	0.551
		Time * Group	8.871	**< .001**	0.388
	Wave V	Time	14.134	**< .001**	0.502
		Group	23.203	**< .001**	0.624
		Time * Group	10.990	**< .001**	0.440
8 kHz	Wave I	Time	8.102	**< .001**	0.367
		Group	14.409	**0.002**	0.507
		Time * Group	11.760	**< .001**	0.457
	Wave III	Time	14.084	**< .001**	0.501
		Group	6.266	**0.025**	0.309
		Time * Group	13.826	**< .001**	0.497
	Wave V	Time	8.545	**< .001**	0.379
		Group	9.859	**0.007**	0.413
		Time * Group	9.346	**< .001**	0.400

16 kHz	Wave I	Time	9.845	**< .001**	0.413
		Group	27.486	**< .001**	0.663
		Time * Group	14.328	**< .001**	0.506
	Wave III	Time	9.845	**< .001**	0.413
		Group	13.048	**0.003**	0.482
		Time * Group	14.328	**< .001**	0.506
	Wave V	Time	8.838	**< .001**	0.387
		Group	20.528	**< .001**	0.595
		Time * Group	10.066	**< .001**	0.418

30dB SL ABR			F	p	η^2_p
Click	Wave I	Time	2.554	**0.019**	0.154
		Group	3.637	0.077	0.206
		Time * Group	2.630	**0.016**	0.158
	Wave III	Time	2.544	0.052	0.154
		Group	1.811	0.200	0.115
		Time * Group	2.720	0.040	0.163
	Wave V	Time	2.568	**0.018**	0.155
		Group	1.479	0.244	0.096
		Time * Group	3.429	**0.003**	0.197
8 kHz	Wave I	Time	3.146	**0.018**	0.183
		Group	6.852e -5	0.994	0.000
		Time * Group	0.200	0.945	0.014
	Wave III	Time	2.432	0.069	0.148
		Group	0.020	0.889	0.001
		Time * Group	1.184	0.328	0.078
	Wave V	Time	1.837	0.136	0.116
		Group	0.361	0.558	0.025
		Time * Group	0.618	0.648	0.042
16 kHz	Wave I	Time	2.325	**0.031**	0.142

	Group	1.046	0.324	0.070
	Time * Group	2.381	**0.027**	0.145
Wave	Time	0.562	0.651	0.039
III				
	Group	1.149	0.302	0.076
	Time * Group	1.930	0.136	0.121
Wave V	Time	1.160	0.338	0.077
	Group	4.905e -4	0.983	0.000
	Time * Group	1.646	0.161	0.105

Simple Main Effects			80 dB SPL			30dB SL		
		Time	Mean square	F	p	Mean Square	F	p
Click	Wave I	day1	13.942	31.329	**< .001**	2.097	8.019	**0.013**
		day4	12.438	30.917	**< .001**	1.843	7.730	**0.015**
		day7	4.081	18.418	**< .001**	0.024	0.102	0.754
		day10	1.601	7.023	**0.019**	0.020	0.127	0.726
		day14	3.180	10.008	**0.007**	0.596	3.044	0.103
		day30	1.517	8.285	**0.012**	0.184	1.829	0.198
		day60	1.013	4.393	0.055	0.102	0.632	0.440
	Wave III	day1	9.708	30.148	**< .001**	1.977	6.629	**0.022**
		day4	5.754	23.070	**< .001**	0.692	3.416	0.086
		day7	3.725	33.967	**< .001**	0.470	3.917	0.068
		day10	1.690	11.712	**0.004**	0.093	0.665	0.429
		day14	0.854	8.587	**0.011**	0.039	0.474	0.502
		day30	0.634	4.714	**0.048**	0.005	0.088	0.771
		day60	0.064	0.315	0.584	0.029	0.219	0.647
	Wave V	day1	17.134	45.066	**< .001**	3.596	9.213	**0.009**
		day4	14.672	35.376	**< .001**	2.178	8.580	**0.011**
		day7	4.419	13.382	**0.003**	0.056	0.132	0.722
		day10	2.264	8.415	**0.012**	0.012	0.043	0.839
		day14	4.709	16.223	**0.001**	0.104	0.347	0.565
		day30	1.214	3.651	0.077	0.009	0.028	0.870

		day60	0.414	1.155	0.301	0.002	0.007	0.934
8 kHz	Wave I	day1	7.136	45.959	**< .001**	0.000	0.004	0.948
		day4	6.915	37.954	**< .001**	0.001	0.014	0.909
		day7	1.892	15.704	**0.001**	0.017	0.551	0.470
		day10	0.754	2.693	0.123	0.014	0.159	0.696
		day14	0.803	4.657	**0.049**	0.010	0.096	0.762
		day30	0.421	2.532	0.134	0.001	0.015	0.904
		day60	0.285	1.562	0.232	0.006	0.450	0.513
	Wave III	day1	5.977	37.898	**< .001**	0.084	0.838	0.375
		day4	4.139	36.832	**< .001**	0.000	0.000	0.984
		day7	3.544	23.802	**< .001**	0.034	0.703	0.416
		day10	0.990	5.847	**0.030**	0.017	0.232	0.637
		day14	0.167	0.851	0.372	0.055	1.274	0.278
		day30	0.022	0.131	0.722	0.041	0.301	0.592
		day60	0.167	0.640	0.437	0.062	1.420	0.253
	Wave V	day1	6.374	100.269	**< .001**	0.020	0.135	0.719
		day4	4.459	28.229	**< .001**	0.005	0.165	0.691
		day7	1.580	11.078	**0.005**	0.129	3.798	0.072
		day10	0.392	2.043	0.175	0.104	1.256	0.281
		day14	0.449	3.269	0.092	0.001	0.010	0.924
		day30	0.006	0.026	0.875	0.018	0.149	0.705
		day60	0.017	0.060	0.811	0.007	0.187	0.672

16 kHz	Wave I	day1	5.090	40.130	**< .001**	0.205	2.470	0.138
		day4	5.910	61.374	**< .001**	0.026	0.827	0.378
		day7	2.397	29.278	**< .001**	0.090	2.321	0.150
		day10	0.723	4.602	0.050	0.009	0.305	0.590
		day14	1.766	24.888	**< .001**	0.009	0.153	0.701
		day30	0.515	6.551	**0.023**	0.000	0.000	0.992
		day60	0.205	2.242	0.156	0.022	1.009	0.332
	Wave III	day1	3.592	39.592	**< .001**	0.205	2.470	0.138
		day4	2.919	38.728	**< .001**	0.026	0.827	0.378
		day7	2.507	35.072	**< .001**	0.090	2.321	0.150
		day10	0.965	11.997	**0.004**	0.009	0.305	0.590
		day14	0.676	8.374	**0.012**	0.009	0.153	0.701
		day30	0.253	3.337	0.089	0.000	0.000	0.992
		day60	0.006	0.056	0.816	0.022	1.009	0.332
	Wave V	day1	4.772	37.802	**< .001**	0.118	1.617	0.224
		day4	3.414	44.163	**< .001**	0.000	0.005	0.945
		day7	2.150	21.095	**< .001**	0.066	1.575	0.230
		day10	0.902	7.214	**0.018**	0.000	0.002	0.961
		day14	1.283	15.210	**0.002**	0.017	0.336	0.571
		day30	0.100	0.888	0.362	0.103	1.301	0.273
		day60	0.019	0.293	0.597	0.079	1.541	0.235

			80dB SPL							30dB SL						
			day1	day4	day7	day10	day14	day30	day60	day1	day4	day7	day10	day14	day30	day60
Click	Wave I	Blast	**<0.001**	**<0.001**	**<0.001**	**<0.001**	**<0.001**	**<0.001**	**<0.001**	**0.001**	0.244	1.000	1.000	1.000	0.300	0.808
		Sham	1.000	1.000	1.000	1.000	1.000	0.984	0.999	1.000	1.000	1.000	1.000	1.000	0.997	1.000
	Wave III	Blast	**<0.001**	**<0.001**	**<0.001**	**<0.001**	**<0.001**	**<0.001**	**0.002**	**0.003**	**0.015**	0.780	0.285	0.934	0.528	0.797
		Sham	1.000	0.916	1.000	0.915	0.902	0.838	0.600	1.000	1.000	1.000	0.966	0.767	0.854	0.652
	Wave V	Blast	**<0.001**	**<0.001**	**<0.001**	**<0.001**	**<0.001**	**<0.001**	**<0.001**	**0.009**	0.440	1.000	1.000	1.000	1.000	1.000
		Sham	1.000	1.000	1.000	1.000	1.000	0.990	0.997	1.000	1.000	1.000	1.000	1.000	0.967	1.000
8 kHz	Wave I	Blast	**<0.001**	**<0.001**	**<0.001**	**0.129**	**0.525**	**0.575**	**0.008**	0.840	0.996	1.000	1.000	1.000	1.000	0.943
		Sha	0.978	1.000	0.998	1.000	1.000	1.000	0.972	0.957	0.999	1.000	1.000	1.000	1.000	1.000

		m														
	Wave III	Blast	**<0.001**	**<0.001**	**<0.001**	**<0.001**	**<0.001**	**<0.023**	0.878	0.998	1.000	1.000	1.000	1.000	1.000	1.000
		Sham	1.000	0.996	1.000	1.000	0.968	1.000	0.999	0.995	1.000	1.000	0.998	0.932	1.000	0.932
	Wave V	Blast	**<0.001**	**<0.001**	**<0.001**	0.993	0.994	1.000	1.000	0.902	1.000	1.000	1.000	1.000	1.000	1.000
		Sham	1.000	1.000	0.991	1.000	1.000	1.000	0.974	1.000	1.000	0.998	1.000	1.000	1.000	0.999
16 kHz	Wave I	Blast	**<0.001**	**<0.001**	**<0.001**	**<0.001**	0.050	**0.020**	**<0.001**	1.000	1.000	1.000	1.000	1.000	1.000	0.999
		Sham	1.000	0.993	0.997	0.965	1.000	1.000	0.149	0.296	0.999	1.000	1.000	1.000	1.000	0.973
	Wave III	Blast	**<0.001**	**<0.001**	**<0.001**	**<0.001**	**<0.001**	**<0.001**	**<0.001**	1.000	1.000	1.000	1.000	0.993	1.000	0.930
		Sham	1.000	0.990	0.973	0.534	0.805	0.838	0.203	1.000	0.982	1.000	0.994	0.880	0.938	0.890

Wave V	Blast	**<0.001**	**<0.001**	**<0.001**	**<0.001**	**0.031**	0.879	0.063	1.000	1.000	1.000	1.000	0.998	1.000	1.000
	Sham	1.000	1.000	0.899	0.520	1.000	0.915	**0.031**	1.000	1.000	1.000	1.000	1.000	0.986	0.843